CAPACITY ANALYSIS OF WIRELESS MULTI-HOP AD HOC ACCESS NETWORKS WITH DIRECTIONAL ANTENNA

Mr. Patrachart Komolkiti

A Dissertation Submitted in Partial Fulfillment of the Requirements
for the Degree of Doctor of Philosophy Program in Electrical Engineering
Department of Electrical Engineering
Faculty of Engineering
Chulalongkorn University
Academic Year 2010

การวิเคราะห์ความจุของโครงข่ายเข้าถึงไร้สายแอดฮอกหลายช่วงเชื่อมต่อ
กับสายอากาศระบุทิศทาง

นายภัทรชาติ โกมลกิติ

วิทยานิพนธ์นี้เป็นส่วนหนึ่งของการศึกษาตามหลักสูตรปริญญาวิศวกรรมศาสตรดุษฎีบัณฑิต
สาขาวิชาวิศวกรรมไฟฟ้า ภาควิชาวิศวกรรมไฟฟ้า
คณะวิศวกรรมศาสตร์ จุฬาลงกรณ์มหาวิทยาลัย
ปีการศึกษา 2553

Thesis Title	CAPACITY ANALYSIS OF WIRELESS MULTI-HOP AD HOC ACCESS NETWORKS WITH DIRECTIONAL ANTENNA
By	Mr. Patrachart Komolkiti
Field of Study	Electrical Engineering
Thesis Advisor	Assistant Professor Chaodit Aswakul, Ph.D.

Accepted by the Faculty of Engineering, Chulalongkorn University in Partial Fulfillment of the Requirements for the Doctoral Degree

. . . . Dean of the Faculty of Engineering
(Associate Professor Boonsom Lerdhirunwong, Dr.Ing.)

THESIS COMMITTEE

. . . . Chairman
(Associate Professor Somchai Jitapunkul, Dr.Ing.)

. . . . Thesis Advisor
(Assistant Professor Chaodit Aswakul, Ph.D.)

. . . . Examiner
(Assistant Professor Tuptim Angkaew, D.Eng.)

. . . . Examiner
(Assistant Professor Chaiyachet Saivichit, Ph.D.)

. . . . External Examiner
(Assistant Professor Kittiphan Techakittiroj, Ph.D.)

ภัทรชาติ โกมลกิติ : การวิเคราะห์ความจุของโครงข่ายเข้าถึงไร้สายแอดฮอกหลายช่วงเชื่อมต่อกับสายอากาศระบุทิศทาง. (Capacity Analysis of Wireless Multi-Hop Ad Hoc Access Networks with Directional Antenna) อ. ที่ปรึกษาวิทยานิพนธ์หลัก : ผศ.ดร. เชาวน์ดิศ อัศวกุล, 56 หน้า.

โครงข่ายไร้สายในอนาคตมุ่งไปที่การบูรณาการการเชื่อมต่อแบบแอดฮอกหลายช่วงเชื่อมต่อ เนื่องด้วยความยืดหยุ่นของวิธีการดังกล่าว สามารถทำให้เกิดการประยุกต์ได้อย่างกว้างขวาง แต่การนำไปใช้งานจริงยังอยู่ในวงแคบ เนื่องจากยังมีประเด็นปัญหาทางเทคนิคที่ยังไม่ได้รับการแก้ไข มีงานวิจัยจำนวนมากพยายามศึกษาประเด็นปัญหาของโครงข่ายแอดฮอกหลายช่วงเชื่อมต่อ ทั้งในด้านการเคลื่อนที่ การเชื่อมต่อ การหาเส้นทาง การจัดกำหนดการ และการควบคุมการเข้าถึงตัวกลาง ถึงกระนั้น ปัญหาของโครงข่ายไร้สายที่ได้รับการสืบทอดมา ก็คือการมีทรัพยากรทางความถี่วิทยุอยู่อย่างจำกัด หนึ่งในเครื่องมือที่สามารถปรับปรุงการใช้ทรัพยากรได้แก่ สายอากาศระบุทิศทาง อันจะนำมาซึ่งการใช้ทรัพยากรและความจุที่ดีขึ้น อย่างไรก็ตาม ผลกระทบที่เกิดขึ้นโดยรวมก็ยังไม่ได้ถูกค้นพบทั้งหมด

วิทยานิพนธ์นี้ มีเป้าหมายที่จะเปิดเผยข้อจำกัดทางกายภาพที่เป็นตัวควบคุมความจุของการสื่อสารแบบแอดฮอกหลายช่วงเชื่อมต่อที่ใช้สายอากาศระบุทิศทาง ผลที่ได้จะนำไปสู่การเพิ่มความจุของโครงข่ายเข้าถึงแอดฮอกหลายช่วงเชื่อมต่อให้สูงสุด กรอบการวิเคราะห์ที่นำเสนอ ได้รวมความสามารถในการลดการรบกวนเชิงพื้นที่ของสายอากาศระบุทิศทางไว้ด้วย จุดเด่นของสูตรที่นำเสนออยู่ที่การใช้การแทนด้วยเวกเตอร์ เมื่อรวมกับแบบจำลองสายอากาศแบบกรวยและลูกกลม ค่าการรบกวนสะสมสามารถถูกแสดงได้อย่างง่ายดายโดยหลักการของตัวรบกวนเทียบเท่า สูตรการคำนวณดังกล่าวได้มีการเปรียบเทียบเชิงเลขกับการจำลองแบบมอนติคาร์โลที่ใช้รูปแบบสายอากาศเสมือนจริงเพื่อการทวนสอบ โดยให้ผลที่สอดคล้องกัน จึงนำมาสู่การกำหนดเงื่อนไขในการให้ค่าที่เหมาะที่สุดในแต่ละมิติของระบบพิกัดเชิงขั้ว เงื่อนไขของมิติมุมอยู่ในรูปของเงื่อนไขการแบ่งแยกขั้นต่ำรอบเกตเวย์ ส่วนเงื่อนไขของมิติระยะอยู่ในรูปของเงื่อนไขการเลือกรีเลย์ที่เหมาะที่สุด ผลที่ได้เป็นแนวทางที่สำคัญต่อการออกแบบโปรโตคอลต่อไป

ภาควิชา วิศวกรรมไฟฟ้า ลายมือชื่อนิสิต
สาขาวิชา วิศวกรรมไฟฟ้า ลายมือชื่อ อ.ที่ปรึกษาวิทยานิพนธ์หลัก
ปีการศึกษา 2553

##4871872421: MAJOR ELECTRICAL ENGINEERING
KEY WORDS: CAPACITY / WIRELESS MULTI-HOP AD HOC ACCESS NETWORK / DIRECTIONAL ANTENNA

PATRACHART KOMOLKITI : CAPACITY ANALYSIS OF WIRELESS MULTI-HOP AD HOC ACCESS NETWORKS WITH DIRECTIONAL ANTENNA, THESIS ADVISOR : ASST. PROF. CHAODIT ASWAKUL, Ph.D., 56 pp.

The future of wireless networks points towards an integration of multi-hop ad hoc connections. The flexibility of the scheme enables a wide range of applications. The implementations, however, are still very limited, as many technical issues remain unsolved. There have been many research works addressing those challenging issues of the wireless multi-hop ad hoc networks, including mobility, connectivity, routing, scheduling, and media access control. Nevertheless, the inherit problems of wireless networks is radio frequency resource scarcity. One of the tools that could improve the resource usage is directional antenna. It can lead to better resource-usage and capacity. The overall effects, however, have not been entirely discovered.

The aim of this dissertation is to disclose the physical constraints that govern the capacity of the multi-hop ad hoc communications equipped with directional antenna. The results shed the light on the capacity maximization of multi-hop ad hoc access networks. The proposed analytical framework integrates the ability to reduce spatial interference of directional antenna. The novelty of the proposed formula is in the usage of the vector representations. Enabled by the cone-plus-ball antenna model, the cumulative interference is found to be conveniently expressed by the concept of equivalent interferers. For verification purpose, the derived formula is also numerically compared to Monte Carlo simulations of realistic antenna patterns, which shows good agreements. Based on the polar coordinate system, the optimal conditions for each dimension are herein derived. The optimal condition for the angle dimension is described as the minimum separable condition around a gateway. The optimal condition for the distance dimension is found as the optimal relay selection condition. The results provide valuable insights to the protocol design.

Department: Electrical Engineering	Student's signature ....
Field of study: Electrical Engineering	Advisor's signature ....
Academic year: 2010	

Acknowledgements

First and foremost, this dissertation would not have been possible without my advisor, Asst. Prof. Dr. Chaodit Aswakul. Throughout the study, he has shown intricacy, resiliency, and sincerity. Those qualities not only allow me to work with ease, but also transform me to be a better scholar. I am forever indebted to his priceless guidance. Furthermore, I am thankful to my informal co-advisor, Asst. Prof. Dr. Chaiyachet Saivichit, for his invaluable comments along the way. It is an honor to me to also have Asst. Prof. Dr. Tuptim Angkaew, my advisor since my Bachelor's degree, as a committee. Her generosity has always been my shining example.

Second, I am grateful to Assumption University for a financial assistance. I also would like to thank the 90^{th} anniversary of Chulalongkorn University fund, TRIDI, and Center of Excellence in Lightwave and High-Speed Communications for the research financial support.

Third, it is a pleasure to thank many of my colleagues in the research lab. Many thanks to my peer, Kalika, who is always helpful for showing me a different perspective. Plenty of thanks to Dr.Vorapoj, Dr.Ajalawit, Pitipong, My, Kamontep and Tri, for their helps in a number of ways. For this occasion, I would like to thank the Master's degree students in the lab too: Panida, Piyanan, Kanin, Sasirom, Veerayuth, Pornpong, Bowornrat, Patcharee, Sunya, Chatkwan, Piangpoon, and many others that might have fallen off my mind. I would not have come to this point without them.

Last, but not least, I owe my deepest gratitude to my family members. The undying support from them has lifted me over countless barriers. My sincerest thank is to my wife, Rattana, for the love and understanding that she has. I would not be able to complete this dissertation without her.

Contents

List of Figures

Figure Page

List of Tables

CHAPTER I

INTRODUCTION

There is no denying that the future of the Internet is pointing towards ubiquity. One of the key components that drives that trend is wireless networks, including cellular networks, Wi-Fi, or the upcoming WiMAX. Nevertheless, even with relative ease of deployment compared to the wired networks, each base station, access point, or generically, *gateway*, still needs a wire to connect to the Internet, and it is not cost-effective to provide such a connectivity. Many research works have been trying to address the problem, and a widely-accepted solution is involving multi-hop ad hoc networks where wired intermediate connections are replaced by wireless multi-hop relaying [1]. This scheme has been recognized as an efficient way to provide connections for networks of the future [2], including vehicular networks, wireless mesh networks, and wireless sensor networks. However, one of the inherit problems of wireless networks is radio frequency resource scarcity. Various techniques have been proposed to improve the *bits per second per hertz* ratio, notably the MIMO technique [3]. Still, the root of the problem is due to the poor *frequency reuse* caused by unnecessary interference of omnidirectional antenna. Thanks to the advances in antenna technology and signal processing, it is now possible to employ *directional antenna* that, potentially, can increase frequency reuse, and, consequently, increase the overall capacity of networks [4].

This dissertation aims to address the capacity of *wireless multi-hop ad hoc access networks with directional antenna* from an analytical point of view. Although there have been other works that describe the capacity of wireless networks, they are assuming uniformly-distributed node-to-node traffic pattern, and pessimistic, i.e., random relay node location [5]. Their results then are usually given as a lower bound. Contrasting to them, this work assumes that traffic patterns are in fact either *from the Internet*, or *to the Internet*, which can be easily justified. Moreover, a criterion in choosing relay nodes that maximize the capacity is proposed. Hence, the capacity is now bounded by the throughput at a gateway. The result is insightful in protocol designing especially in the multi-hop scenarios.

1.1 Literature Review

This dissertation focuses on three research areas, namely, *capacity of wireless networks*, *wireless ad hoc access networks*, and *effects of directional antenna*. This section reviews the relevant research works.

1.1.1 Capacity of Wireless Networks

The capacity of wireless networks has been widely investigated since the seminal work of P. Gupta and P. R. Kumar [5]. For general wireless networks with adjustable transmission range, the work describes the relationship between the number of nodes in an area and the upper bound of transport capacity, in the unit of bit-meter per second. In particular, the relationship, using the Bachmann-Landau notation, is shown as the scaling laws [6] where per-node throughput varies with the number of nodes in the network n and channel capacity W. In the random node-placement scenario, the per-node throughput is $\Theta(\frac{W}{\sqrt{n \log n}})$, where $\Theta(.)$ is defined as the asymptotic bound of exact order [7]. In the best-case scenario, the per-node throughput is $\Theta(\frac{W}{\sqrt{n}})$ and the resulting total capacity is $\Theta(W\sqrt{n})$. Comparing with a common wireless channel with the total capacity of $\Theta(W)$, these results suggest that *spatial reuse* can occur. One of the important notions from [6] is a concept of *exclusion disk*, which is defined as an area of a circle with radius $\frac{\Delta}{2}$ times the transmission range, centered at each receiver. What that notion, concurrent transmissions are possible only when the respective exclusion disks are disjoint. This can be viewed as a receiver-based interference model. Note that the concept of exclusion disks is not directly applicable for half duplex transmissions protocols, such as IEEE 802.11. In half duplex communications, each receiving node also acts as a transmitter node, and vice versa. The definition of receiver-based exclusion zone then becomes invalid.

The groundbreaking work in [5] inspires many follow-up works. J. Li, C. Blake, D. S. J. D. Couto, H. I. Lee, and R. Morris [8] considered the effect of different traffic patterns on the scalability of per node capacity. They showed that the random traffic pattern from [5] offers the pessimistic view, and introduced a power-law traffic pattern that is more scalable. The result implies that, while multi-hop ad hoc networks provide better coverage, there should be a limit of the maximum number of hops that does not degrade the total network throughput.

K. Jain, J. Padhye, V. N. Padmanabhan, and L. Qiu [9] formulated a *conflict graph* to represent link-pair interference and used it as a constraint for scheduling, which reflects the throughput. They claimed that it is NP-hard to approximate the optimal throughput and proposed heuristic approaches to find the lower and upper bounds on the optimal throughput. They also suggested that, by reducing *sending rate* while maintaining connectivity, it is possible to improve the scalability of the per-node throughput.

T.-S. Kim, H. Lim, and J. C. Hou [10] focused on reducing unnecessary interference and maximizing spatial reuse of omnidirectional multi-hop wireless networks with a power control method that adjusts transmission power and carrier sense threshold. Their proposed algorithm is verified by simulations.

A. Zemlianov and G. de Veciana [11] inserted additional infrastructure nodes, which are interconnected by uninterfered alternative links. The traffic are node-to-node based. The additional nodes do not generate any traffic themselves and are used purely for relaying. Their result demonstrates the effect of the number of infrastructure nodes m on the number of ad hoc nodes n. In particular, when m is less than $\sqrt{\frac{n}{\log n}}$, there is no capacity improvement. J.-W. Cho, S.-L. Kim, and S. Chong [12] extended the work of [11] by replacing the simplified protocol interference model with a more complicated physical interference model.

The throughput of a data-gathering wireless sensor network, which is architecturally similar to single-access-point wireless ad hoc access networks, with omnidirectional transmissions, has been derived by E. J. Duarte-Melo and M. Liu [13]. The approaches from [5] and [13] have been used by C. P. Chan and S. C. Liew [14] with additional constraints of IEEE 802.11-like MAC protocol and a fixed topology. The result is found as a bound of capacity experienced at the sink node.

P. C. Ng, S. C. Liew, and L. B. Jiang [15], [16], and [17] described the impact of IEEE 802.11 physical and protocol interferences on capacity, and showed that the total network capacity does not scale with the node density, which reflects the need for better technique in dealing with unnecessary interferences.

P. C. Ng and S. C. Liew [18] extended the analysis of IEEE 802.11 interferences to a specific case of single-flow evenly-spaced multi-hop network with basic access mode. They concluded that hidden-node effect dominates the sustainable throughput, and the more the potential hidden nodes, the smaller the achievable throughput.

1.1.2 Wireless Multi-hop Ad Hoc Access Networks

With the rise in popularity of wireless LANs, a natural progress of the technology is to provide a better coverage while maintaining its unlicensed status. Y.-C. Tseng, C.-C. Shen, and W.-T. Chen [1] suggested an architecture of multi-hop ad hoc networks that could provide better coverage for Internet connections, possibly with multiple gateways, and integrated mobile ad hoc networks to the existing mobile IP scheme. U. Jönsson, F. Alriksson, T. Larsson, P. Johansson, and G. Q. Maguire [2] proposed *MIPMANET* that extends the normal mobile IP to allow ad hoc connectivity. T.-C. Huang and S.-Y. Wu [19] incorporated a gateway discovery algorithm to the mobile IP scheme, while E. Nordström, P. Gunningberg, and C. Tschudin [20] concentrated on the forwarding mechanism of IP in ad hoc access networks. As a comparison, H. M. Ammari [21] used simulations with several settings and scenarios to study the effectiveness of the ad hoc access network scheme. P. M. Ruiz, F. J. Ros, and A. Gomez-Skarmeta [22] also applied several network-layer schemes over ad hoc access networks to simulations, and the results are shown in terms of overhead, delay, and packet delivery ratio.

Specific routing techniques have also been discussed. J. H. Song, V. W. S. Wong, and V. C. M. Leung [23] proposed a routing protocol for mobile multi-hop ad hoc access networks by logical partitioning based on the assumption that traffic is either going to or coming from the gateway. C.-F. Huang, H.-W. Lee, and Y.-C. Tseng [24] extended the concept of load balancing in routing for the case of multiple gateways.

C.-Y. Hsu, J.-L. C. Wu, and S.-T. Wang [25] argued that the multi-hop ad hoc access networks could suffer from a downstream congestion because of extensive contentions of CSMA/CA, and proposed a modification of the CSMA-based MAC protocol to improve the capacity of multi-hop ad hoc access networks.

Gateway placement has been considered by P. Zhou, X. Wang, and R. Rao [26], and asymptotic capacity of infrastructure wireless mesh networks has been derived. Omnidirectional mesh nodes, with and without gateway capability, are placed according to a square-grid formation, and the proper mixture of the number of gateways and the number of relay nodes are derived to maximize the per-node throughput.

1.1.3 Directional Antenna

Due to advancement in antenna technology and scarcity of wireless resources, there have been many studies on the topic of directional antenna that potentially could provide better spatial reuse, ranging from protocol design, implementations, and capacity analysis.

Many researchers have been paying attention to the redesign of MAC protocols to support the new physical layer specification, as it can be seen in a survey work by R. Vilzmann and C. Bettstetter [4]. One of the aspects that must be carefully considered is the notion of *deafness* [27], where improper protocol may cause nodes to be unaware of the situation because they are directionally concentrating on their own communications. R. R. Choudhury and N. H. Vaidya [28] also observed the impacts of directional antenna on routing protocols. R. Ramanathan, J. Redi, C. Santivanez, D. Wiggins, and S. Polit [29] performed experiments of mobile ad hoc networks with directional antenna, which show promising results. Note that all these works use *improvements* as a key result, while the bounds of performance are still to be studied.

Y. Hua, Y. Huang, and J. Garcia-Luna-Aceves [30] studied wireless networks on a square grid, with directional antenna capability. The work uses a simplified directional antenna model since all nodes are aligning on a grid. The optimal scheduling that yields maximum capacity is numerically obtained.

To mimic the technique of calculating maximum throughput of wire-line networks by using min-cut/max-flow theorem, C. Peraki and S. D. Servetto [31] formed a special case of wireless networks with directional antenna by placing source nodes on one side of an area, destination nodes on the other non-overlapping side of the same area. By counting how many cross-the-border edges can be constructed simultaneously between sources and destinations, the number of concurrent transmissions can be determined.

R. Ramanathan [32] proposed a *hybrid* antenna model, which is often referred to as *cone-plus-ball* model, to capture the side-lobe effect in a tractable fashion.

O. Bazan and M. Jaseemuddin [33] considered the more realistic antenna models and used the corresponding conflict graph to formulate a linear programming problem. Numerical results show that the effect of side lobes cannot be neglected, but the impact has not been analytically explained.

A direct extension of [5] with directional antenna has been done by A. Spyropoulos and

C. S. Raghavendra [34], [35], and later more extensively by S. Yi, Y. Pei, S. Kalyanaraman, and B. Azimi-Sadjadi [36]. The works follow the same steps as [5], though the results are purely theoretical and do not consider the half-duplex nature of MAC protocols.

1.2 Objective of Dissertation

The objective of this dissertation is to propose a general analytical framework for wireless multi-hop ad hoc access networks with directional antenna capability. Maximum throughput obtained from the proposed method is applicable even with the random node placement, overcoming the usual problem of numerical methods. The results can give insights to the design of MAC protocol, routing, and scheduling.

1.3 Scope of Dissertation

The scope of this dissertation in investigating the capacity of wireless ad hoc access networks with directional antenna is described as follows.

1. Study the wireless network capacity analysis techniques.

2. Generalizing the fundamental constraints of wireless networks to include the effect of directional antenna.

3. Study the effects of the proposed method and provide a comparative study with the other omnidirectional and directional schemes.

4. Develop a computer program to numerically analyze the method.

5. Propose criteria that maximize the overall capacity of wireless multi-hop ad hoc access networks.

1.4 Synopsis of Dissertation

After the introduction in this chapter, the general background of the analytical framework is explained in **Chapter II**. Capacity analysis of wireless networks are shown both for the condition-based throughput and the Shanon capacity. The basic of analytically tractable directional antenna model is also covered here and to be used throughout the dissertation.

The combination of the reception conditions and directional antenna is explored in **Chapter III**. Here, the Protocol Model becomes complicated, as there is an extra dimension of direction to consider. Uniquely, the vector representation of the conditions is proposed, resulting in a unified constraint for simultaneous communications using directional antenna. Those conditions are applied to a structure of homogeneous ad hoc access network with symmetrical node placement around a gateway. The other contribution from this chapter is the notion of minimum separation angle, defined as the minimum angle around a single gateway that each concurrent communicating pairs can coexist. Based on the polar coordinate system, this is the optimal condition for the angle dimension. Maximum throughput can then be achieved by optimal scheduling that fully utilizes the gateway.

To fully reach the limitation of capacity, the reception conditions are relaxed and concentration is on the maximum-possible capacity. Capacity bound based on Shannon capacity for networks of nodes equipped with directional antenna is investigated in **Chapter IV**. Specifically, the emphasis is on a single hop communication in a homogeneous environment that has other concurrent transmissions uniformly distributed on 2-dimensional plane. Those concurrent transmitters act as interferers from the intended receiver's point of view. The contribution is found in terms of equivalent interferers as a function of node activity ratio. The analytical result is verified by comparing with simulations of nodes with realistic antenna pattern. The effect of varying node activity ratio and beamwidth are also shown.

Extension of Chapter IV to include the possibility of multi-hop communications is considered in **Chapter V**. A special case of multi-hop ad hoc access networks, namely, a 1-dimensional network, is considered. The results are shown in terms of end-to-end capacity and network capacity. Interestingly, the maximum capacity can be obtained by selecting the best distance for each hop of relaying, regardless of the distance of the destination. The only factor is the loss exponent of the environment. Based on the polar coordinate system, this is the optimal condition for the distance dimension. The contributions from this chapter then complements the contributions obtained from Chapter III. The results here give insights to the protocol design.

The dissertation is finally concluded in **Chapter VI**, together with suggestion for possible future work.

CHAPTER II

FUNDAMENTAL CONCEPT OF CAPACITY ANALYSIS AND DIRECTIONAL ANTENNA

This chapter describes the basic concept of wireless network capacity analysis. Two kinds of capacity are considered in this dissertation: throughput based on reception conditions for a given data rate in Section 2.1 and Shannon capacity in Section 2.2. The basic of directional antenna considered in networking context is also covered in Section 2.3. In the following derivations, a homogeneous transmission power level P, noise power level N, bandwidth BW, and path loss exponent α are assumed unless specified.

2.1 Reception Conditions for a Constant Data Rate

The concept of capacity in this scheme is directly based on the maximum throughput, which measures the *successful* transmissions. Whether a transmission is successful is commonly indicated by constraints. The two models used to govern these constraints are called the *Physical Model* and the *Protocol Model* [5].

In the Physical Model, a common requirement of successful communications, stemmed from the receiver design, is a minimum *Signal-to-Interference Ratio*, or *SIR*, denoted by ξ. Following the notation used in [5], let X_i denote a node and its position, $H_{X_iX_j}$ denote an antenna gain between X_i and X_j, and $\mathbf{T}$ denote a set of simultaneously transmitting nodes. Then, X_j can successfully receive a transmission from X_i, when other nodes $X_k \in \mathbf{T}$ are also transmitting, if

$$\frac{\dfrac{H_{X_iX_j}P}{|X_i - X_j|^\alpha}}{N + \displaystyle\sum_{k\in\mathbf{T},k\neq i} \dfrac{H_{X_kX_j}P}{|X_k - X_j|^\alpha}} \geq \xi. \tag{2.1}$$

On the other hand, a successful wireless communication can also be viewed as depending on a *transmission range* r, which represents the maximum value of $|X_i - X_j|$ that satisfies (2.1) in a case where $\mathbf{T} = \{X_i\}$. With omnidirectional antenna, r is usually considered to be a fixed value. In this case, simplified from (2.1), X_i may communicate with X_j if

$$|X_i - X_j| \ \leq r. \tag{2.2}$$

However, whether a transmission is successful also depends on interference. From (2.1), X_k does not interfere the reception at X_j from the transmission of X_i if

$$\frac{\dfrac{H_{X_iX_j}P}{|X_i - X_j|^\alpha}}{N + \dfrac{H_{X_kX_j}P}{|X_k - X_j|^\alpha}} \geq \xi. \tag{2.3}$$

Assuming that N is relatively negligible [14], [18], [30], [37], with omnidirectional antenna normalized gain $H_{X_iX_j} = 1$, (2.3) becomes

$$\frac{|X_k - X_j|}{|X_i - X_j|} \geq \sqrt[\alpha]{\xi}. \tag{2.4}$$

Inequality (2.4) then can be expressed as

$$|X_k - X_j| \ \geq (1 + \Delta)|X_i - X_j|, \tag{2.5}$$

where Δ is called *guard zone* [5], or *distance margin* [14]. A typical value of Δ is given by [14] for the case of $\alpha = 4$ and $\xi = 10$ dB,

$$\Delta = \sqrt[\alpha]{\xi} - 1 = \sqrt[4]{10} - 1 \approx 0.78. \tag{2.6}$$

Note that, for the case of fixed transmission range, [5] simplifies (2.5) to be

$$|X_k - X_j| \ \geq (1 + \Delta)r. \tag{2.7}$$

Inequality (2.5), or the combination of (2.2) and (2.7), $\forall X_k \in \mathbf{T}$, are called the *Protocol Model*. It reflects the *layer 2* condition that, before X_j can receive the transmission from X_i, the receiver node X_j must not hear any transmissions from any potentially interfering nodes $X_k \in \mathbf{T}$. Note that it is a pair-wise condition. From the Protocol Model, the capacity of wireless networks then depends on how many simultaneously communicating node pairs can occur, without substantially interfering each other. Thus, in an omnidirectional half-duplex protocol like IEEE 802.11, where each node in a communicating node pair alternately acts as a transmitter and a receiver, the conditions for node pairs (X_1, Y_1) and (X_2, Y_2) to be simultaneously communicating are [5], [14], [17]:

$$\begin{aligned}
|X_2 - Y_1| &\geq (1+\Delta)\,|X_1 - Y_1|, \\
|Y_2 - Y_1| &\geq (1+\Delta)\,|X_1 - Y_1|, \\
|X_2 - X_1| &\geq (1+\Delta)\,|Y_1 - X_1|, \\
|Y_2 - X_1| &\geq (1+\Delta)\,|Y_1 - X_1|, \\
|X_1 - Y_2| &\geq (1+\Delta)\,|X_2 - Y_2|, \\
|Y_1 - Y_2| &\geq (1+\Delta)\,|X_2 - Y_2|, \\
|X_1 - X_2| &\geq (1+\Delta)\,|Y_2 - X_2|, \\
|Y_1 - X_2| &\geq (1+\Delta)\,|Y_2 - X_2|.
\end{aligned} \tag{2.8}$$

Inequalities (2.8) are then used as either conditions in deriving maximum number of simultaneously communicating node pairs [5], [14], or constraints in linear programming [31], [33]. However, (2.8) are derived from an assumption that the transmission is omnidirectional. When directional antenna is applied, the relationship is no longer in *scalar* form, but becomes *vector* form, to be elaborated in Section 3.1.

2.2 Shannon Capacity

For an advanced technique of adaptive modulation and coding (AMC), each node pair can adjust the transmission rate according to the situation. Thus, the reception conditions are changed for each adjustment. Instead of dealing with a set of multiple-rate conditions, an upper bound of transmission rate can be specified. For any communicating node pair, the Shannon Capacity theorem gives the upper bound of the transmission rate between the two nodes in a given environment. Thus, a reception capacity $C^{\mathbf{T}}_{X_iX_j}$ of a receiver X_j from a transmitter X_i when other nodes $X_k \in \mathbf{T}$, $k \neq i$ are also transmitting is given by

$$C^{\mathbf{T}}_{X_iX_j} = BW \log_2 \left(1 + \frac{\dfrac{H_{X_iX_j}P}{|X_i - X_j|^{\alpha}}}{N + \displaystyle\sum_{k\in\mathbf{T},k\neq i} \frac{H_{X_kX_j}P}{|X_k - X_j|^{\alpha}}} \right). \tag{2.9}$$

Equation (2.9) exemplifies that the capacity not only depends on the received power from the intended transmitter, but also suffers collectively from the other transmitters of other communications. Thus, calculating the interference power becomes a key point in the analysis. Equation (2.9) also implies that finding a way to reduce the interference can directly impact the capacity.

On the other hand, one must be aware that (2.9) is the bound of just one node-pair. Other node-pairs may be viewed as interferers, but they are in fact having communications of their own. Thus, by reducing the number of node-pairs, each pair may achieve a higher capacity. But that means there are fewer concurrent transmissions. The overall effect must be carefully observed. That effect is considered in Section 5.3.

2.3 Directional Antenna

Directional antenna refers to a type of antenna that intentionally has higher gain in certain directions in the scope of consideration, in comparison with the omnidirectional antenna. An isotropic antenna is a perfect omnidirectional antenna. While a simple dipole antenna can be considered a directional antenna in 3-dimensional space, in 2-dimensional plane it becomes omnidirectional. This dissertation limits the scope to 2-dimensional plane. The beamwidth is then broadly defined as the width of the main beam angle with the intended higher gain. In practice, the beamwidth is specifically called -3dB beamwidth, because higher gain commonly means more than half of the highest gain at the boresight direction.

Table 2.1 List of notations used in directional antenna derivations

Symbol	Description
ϕ_{X_i}	Orientation of X_i
ψ_{X_i}	Active antenna beam direction of X_i relative to ϕ_{X_i}
$\theta(\psi_{X_i})$	Set of active beam angles of X_i with direction ψ_{X_i}
φ_{X_i}	Beamwidth of X_i
η_{X_i}	Efficiency of directional antenna of X_i
B_{X_i}	The number of antenna beams of X_i in non-overlapping switched-beam case

Directional antenna in literature comes in several configurations in terms of physical builds and beamforming techniques. However, with applications in ad hoc networks, the directional antenna can be categorized into 2 main kinds [32]: *switched-beam* antenna and *steered-beam* antenna. Notations as in Table 2.1 are used in directional-antenna formulations and derivations throughout the dissertation. Assuming that the nodes are homogeneous, then $B_{X_i} = B, \varphi_{X_i} = \varphi, \eta_{X_i} = \eta, \forall X_i$.

Switched-beam antenna refers to a type of antenna that can only point towards a set of fixed angles. Normally, it is achieved by using multiple physically-fixed-beam directional antennas, although beamforming can also achieve this. To have the $360°$ coverage as commonly required in ad hoc network applications in allowing communications to nodes at an arbitrary angle, beams are equally and evenly spaced, and the number of beams depends on the beamwidth of each beam to cover all the angles. In operation, a node must determine a direction of transmission/reception and *switches on* an appropriate beam. For B-beams, non-overlapping switched-beam antenna,

$$\varphi = \frac{2\pi}{B} - \eta, \tag{2.10}$$

$$\theta(\psi_{X_i}) = \left\{\theta : \phi_{X_i} + \psi_{X_i} - \frac{\varphi}{2} \leq \theta \leq \phi_{X_i} + \psi_{X_i} + \frac{\varphi}{2}\right\},$$

$$\psi_{X_i} \in \left\{0, \frac{2\pi}{B}, \frac{4\pi}{B}, \ldots, \frac{2(B-1)\pi}{B}\right\}. \tag{2.11}$$

For steered-beam antenna, the boresight of antenna can be *steered* to virtually any direction, usually by beamforming techniques. In practice, the boresight is pointed directly towards the corresponding node in communication for maximum gain, as is also assumed in this dissertation. With beamwidth φ,

$$\theta(\psi_{X_i}) = \left\{\theta : \phi_{X_i} + \psi_{X_i} - \frac{\varphi}{2} \leq \theta \leq \phi_{X_i} + \psi_{X_i} + \frac{\varphi}{2}\right\}, \ \psi_{X_i} \in [0, 2\pi). \tag{2.12}$$

For analytical tractability, a single main-beam hybrid antenna model [32] is considered throughout this dissertation. This model is also referred to as *cone-plus-ball* and widely used in literature [34], [38]. This model captures the effect of directional antenna by representing the main-lobe of antenna pattern with beamwidth φ as *cone* with gain G_m, and side-lobe of antenna pattern as *ball* with gain G_s. Although this model is not as precise as any actual antenna pattern, it still maintains the effect of side-lobe that must not be ignored. Figure 2.1 shows an example of a node X_i with cone-plus-ball antenna pattern with gain G_{X_i}.

For the case of a perfect steered-beam cone-plus-ball antenna, where the main lobe can be pointed virtually in any direction, and normally pointed directly at the corresponding node, the gain can be specified as

$$G_{X_i}(\theta) = \begin{cases} G_M, & \text{if } \theta \in \theta(\psi_{X_i}), \\ G_S, & \text{otherwise,} \end{cases} \tag{2.13}$$

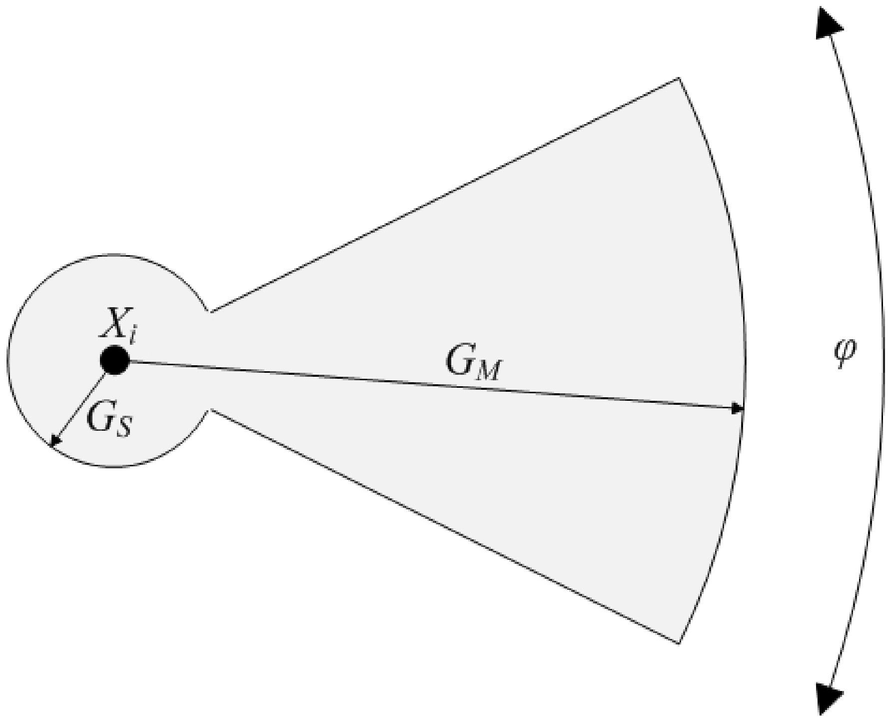

Figure 2.1 Cone-plus-ball antenna pattern

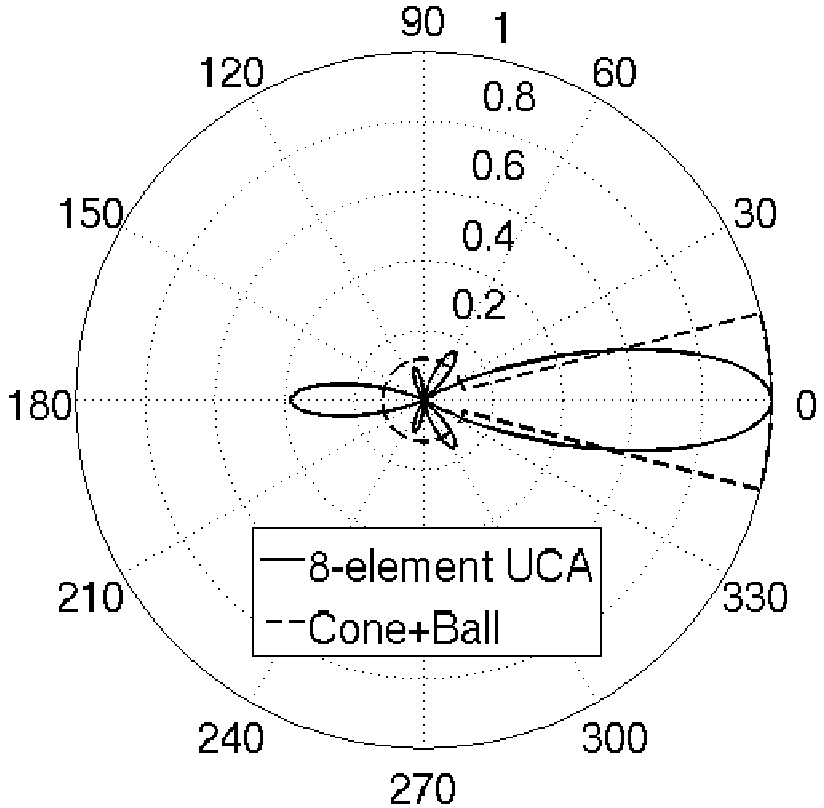

Figure 2.2: Antenna pattern of normalized 8-element UCA antenna and 30°-beamwidth cone-plus-ball model

where G_M and G_S are gains of the main lobe and side lobe, respectively.

In practice, the value of G_M, G_S, and φ are chosen to match the real antenna pattern. Consider the uniform circular array (UCA) [39] as an example of realistic directional antenna pattern. Without loss of generality, the 8-element UCA antenna model is compared to $30°$-beamwidth cone-plus-ball antenna model, where the value of beamwidth is chosen to match the $-3dB$ beamwidth of the UCA. Their beam patterns are shown in Figure 2.2.

Although the antenna patterns do not exactly matched, the benefit of using the cone-plus-ball antenna model is in its analytical tractability. The errors in terms of capacity when using the simplified model, compared to the realistic model, is discussed in Section 4.2.

2.4 Concluding Remarks

In this chapter, the basic formulas in analyzing the capacity of wireless networks are shown in Section 2.1 and Section 2.2. The directional antenna framework is also discussed in Section 2.3. These knowledge are in bits and pieces. Therefore, putting these analyses together in a meaningful way can provide many insights. The combination of the directional antenna and the conditions from Section 2.1 is the focus of Chapter III, under the context of multi-hop ad hoc access networks. Application of the directional antenna to the bound from Section 2.2 leads to the discussion in Chapter IV.

CHAPTER III

MAXIMIZATION OF CONCURRENT TRANSMISSIONS IN SINGLE-GATEWAY WIRELESS MULTI-HOP AD HOC ACCESS NETWORKS WITH DETERMINISTIC NODE PLACEMENT

This chapter describes the proposed framework in analyzing and maximizing capacity of wireless ad hoc access networks with directional antenna based on a reception condition for a constant data rate. A single main-beam hybrid antenna model [32] is considered in this dissertation. The difference to the omnidirectional transmissions is, since each antenna is modeled as *cone-plus-ball*, then there are 2 antenna gains, main-lobe gain G_M and side-lobe gain G_S. Consequently, the concept of *range* has to be modified. Section 3.1 covers the derivation of modified conditions to take into account the effect of directional antenna. The unified conditions from Section 3.1 are applied to a single gateway multi-hop access network in Section 3.2. The main finding is shown in terms of minimum separable condition as a function of antenna beamwidth. By satisfying such the condition, the maximum throughput can then be achieved by simple scheduling because all node-pairs can transmit simultaneously. The chapter is concluded in Section 3.3

3.1 Derivation of Reception Conditions for Networks with Directional Antenna

Recall the Physical Model from Section 2.1, which assumes the homogeneous omnidirectional transmissions with normalized antenna gain. When the cone-plus-ball model is applied, $H_{X_iX_j}$ has to be substituted by proper gains. Consider the scenario as in Figure 3.1 which shows the locations of nodes and their respective antenna patterns. Adapting the same rationale of (2.3)-(2.5) of the Protocol Model, X_j can successfully receive a transmission from X_i while X_{k_1}, X_{k_2}, and X_{k_3} are concurrently transmitting when the following are true:

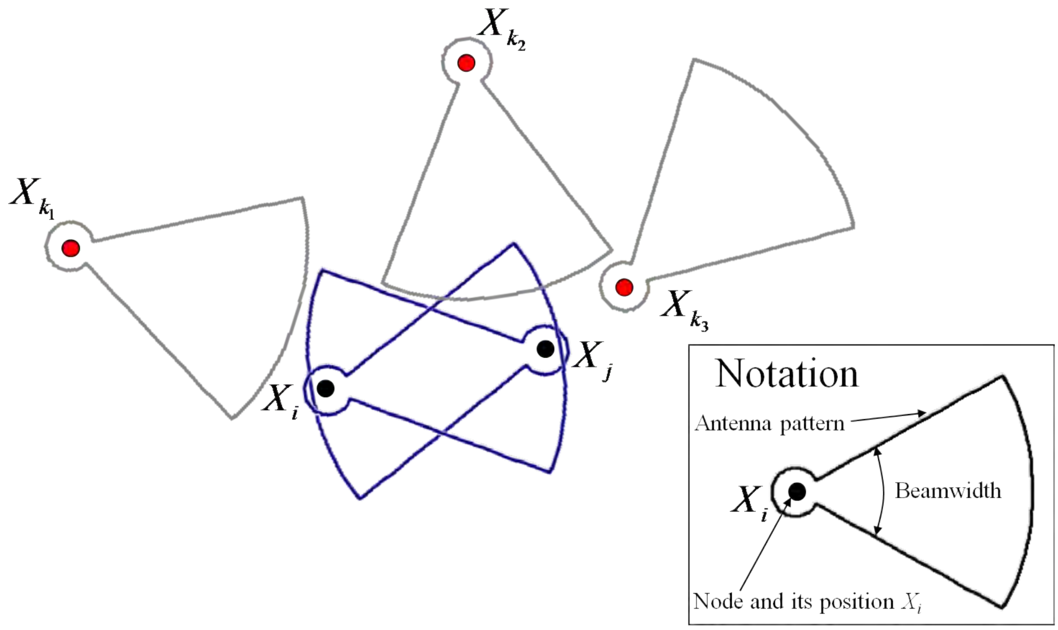

Figure 3.1 Possible communications of nodes equipped with directional antenna

$$\frac{\dfrac{G_M^2 P}{|X_i - X_j|^\alpha}}{\dfrac{G_M^2 P}{|X_{k_1} - X_j|^\alpha}} \geq \xi, \tag{3.1}$$

$$\frac{\dfrac{G_M^2 P}{|X_i - X_j|^\alpha}}{\dfrac{G_M G_S P}{|X_{k_2} - X_j|^\alpha}} \geq \xi, \tag{3.2}$$

$$\frac{\dfrac{G_M^2 P}{|X_i - X_j|^\alpha}}{\dfrac{G_S^2 P}{|X_{k_3} - X_j|^\alpha}} \geq \xi. \tag{3.3}$$

The denominators of (3.1)-(3.3) then can be classified as, *main-lobe-to-main-lobe* interference, *main-lobe-to-side-lobe* interference, and *side-lobe-to-side-lobe* interference, respectively. Similar to (2.3)-(2.5), (3.1)-(3.3) can then be written as

$$|X_{k_1} - X_j| \geq (1 + \Delta_{MM})|X_i - X_j|, \tag{3.4}$$

$$|X_{k_2} - X_j| \geq (1 + \Delta_{MS})|X_i - X_j|, \tag{3.5}$$

$$|X_{k_3} - X_j| \geq (1 + \Delta_{SS})|X_i - X_j|, \tag{3.6}$$

where

$$\Delta_{MM} = \sqrt[\alpha]{\xi} - 1, \tag{3.7}$$

$$\Delta_{MS} = \sqrt[\alpha]{\frac{G_S}{G_M}\xi} - 1, \tag{3.8}$$

$$\Delta_{SS} = \sqrt[\alpha]{\left(\frac{G_S}{G_M}\right)^2 \xi} - 1, \tag{3.9}$$

denoting main-lobe-to-main-lobe distance margin, main-lobe-to-side-lobe distance margin (or, equivalently, side-lobe-to-main-lobe distance margin), and side-lobe-to-side-lobe distance margin, respectively. Note that $\Delta_{MM} > \Delta_{MS} > \Delta_{SS}$. Figure 3.2 illustrates the interference zones of a node X_i with directional antenna. The meaning of each range in Figure 3.2 is as follows: r is the main-lobe-to-main-lobe transmission range, $(G_S/G_M)r$ is the side-lobe-to-side-lobe transmission range (which is not used in the scope of this work), $(1+\Delta_{MM})r$ is the main-lobe-to-main-lobe interference range, $(1+\Delta_{MS})r$ is the main-lobe-to-side-lobe interference range, and $(1+\Delta_{SS})r$ is the side-lobe-to-side-lobe interference range.

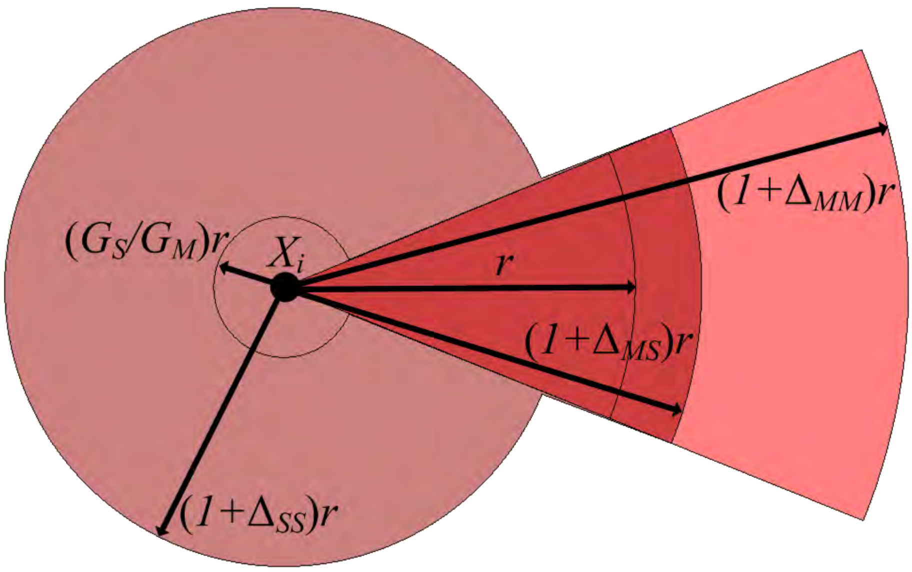

Figure 3.2 Interference zones of a node with directional antenna

The usage of a particular interference zone depends on the antenna directions. For instance, consider Figure 3.1 again. For X_j to be interfered by X_{k_1}, then the main-lobe-to-main-lobe interference zone of X_{k_1} must cover X_j, because the main lobe of X_{k_1} and X_j

are pointing to each other. On the other hand, for X_j to be interfered by X_{k_2}, then the main-lobe-to-side-lobe interference zone of X_{k_2} must cover X_j, because the main lobe of X_{k_2} is pointing to the side lobe of X_j. Note that the main-lobe-to-main-lobe interference zone of X_{k_2} may cover X_j, but that does not cause enough interference according to the Protocol Model.

From the above example, it can be seen that interference conditions are now depending on not only the distance between nodes, but also the *relative antenna directions* of nodes of interest. This clearly shows the needs for vector representations.

To formulate the general conditions of concurrent transmissions with directional antenna, the following notations are used. Let $\overrightarrow{X_iX_j}$ be a vector starting at X_i and ending at X_j. Define

$$\vec{e}_{X_i} = 1\angle\phi_{X_i} \tag{3.10}$$

as a unit vector of X_i's alignment, and define *indicator function* $\mathbf{1}\{.\}$, where

$$\mathbf{1}\{A\} = \begin{cases} 1, & \text{if } A \text{ is true,} \\ 0, & \text{if } A \text{ is false.} \end{cases} \tag{3.11}$$

Using the Protocol Model with half-duplex transmissions and fixed range r, define

$$M^{C}_{X_iX_j} = \mathbf{1}\left\{\|\overrightarrow{X_iX_j}\| \leq r\right\}, \tag{3.12}$$

$$M^{I_{MM}}_{X_iX_j} = \mathbf{1}\left\{\|\overrightarrow{X_iX_j}\| \leq (1+\Delta_{MM})r\right\}, \tag{3.13}$$

$$M^{I_{MS}}_{X_iX_j} = \mathbf{1}\left\{\|\overrightarrow{X_iX_j}\| \leq (1+\Delta_{MS})r\right\}, \tag{3.14}$$

$$M^{I_{SS}}_{X_iX_j} = \mathbf{1}\left\{\|\overrightarrow{X_iX_j}\| \leq (1+\Delta_{SS})r\right\}, \tag{3.15}$$

to indicate whether X_i and X_j are in the communication range, the main-lobe-to-main-lobe interference range, the main-lobe-to-side-lobe interference range, and the side-lobe-to-side-lobe interference range, respectively. Furthermore, since relative antenna directions must be considered, define

$$D_{X_iX_j} = \mathbf{1}\left\{\cos^{-1}\left[\frac{\overrightarrow{X_iX_j}\cdot\vec{e}_{X_i}}{\|\overrightarrow{X_iX_j}\|}\right] \in \theta(\psi_{X_i})\right\}, \tag{3.16}$$

to indicate whether X_j is in the main-beam direction of X_i. It is worth mentioning that $D_{X_iX_j} \neq D_{X_jX_i}$.

By using (3.12) and (3.16), (2.2) can be redefined to include the *direction*. Thus, for node-pair (X_1, Y_1) to communicate, they must be within the communication range and in the main-beam directions of each other, i.e.,

$$M^{C}_{X_1Y_1} \wedge D_{X_1Y_1} \wedge D_{Y_1X_1} = 1. \tag{3.17}$$

For another node-pair (X_2, Y_2) to communicate, then

$$M^{C}_{X_2Y_2} \wedge D_{X_2Y_2} \wedge D_{Y_2X_2} = 1. \tag{3.18}$$

Equations (3.17) and (3.18) imply that only communications via main-beams are considered, and side-beam communications are not allowed. However, for node pairs (X_1, Y_1) and (X_2, Y_2) to communicate simultaneously, their transmissions must not interfere each other. Based on (3.4)-(3.6), and using (3.13)-(3.16), simultaneous communications between node pairs (X_1, Y_1) and (X_2, Y_2) must satisfy

$$\begin{aligned}
&(M^{I_{MM}}_{X_1X_2} \wedge D_{X_1X_2} \wedge D_{X_2X_1}) \vee (M^{I_{MS}}_{X_1X_2} \wedge (D_{X_1X_2} \vee D_{X_2X_1})) \vee M^{I_{SS}}_{X_1X_2} \vee \\
&(M^{I_{MM}}_{Y_1Y_2} \wedge D_{Y_1Y_2} \wedge D_{Y_2Y_1}) \vee (M^{I_{MS}}_{Y_1Y_2} \wedge (D_{Y_1Y_2} \vee D_{Y_2Y_1})) \vee M^{I_{SS}}_{Y_1Y_2} \vee \\
&(M^{I_{MM}}_{X_1Y_2} \wedge D_{X_1Y_2} \wedge D_{Y_2X_1}) \vee (M^{I_{MS}}_{X_1Y_2} \wedge (D_{X_1Y_2} \vee D_{Y_2X_1})) \vee M^{I_{SS}}_{X_1Y_2} \vee \\
&(M^{I_{MM}}_{X_2Y_1} \wedge D_{X_2Y_1} \wedge D_{Y_1X_2}) \vee (M^{I_{MS}}_{X_2Y_1} \wedge (D_{X_2Y_1} \vee D_{Y_1X_2})) \vee M^{I_{SS}}_{X_2Y_1} = 0.
\end{aligned} \tag{3.19}$$

Distinctively, all interference-related conditions are combined into (3.19). It implies that each node pair that is not the communicating pairs must not *see* each other, either by pointing main beams directly at each other ($(M^{I_{MM}}_{X_iX_j} \wedge D_{X_iX_j} \wedge D_{X_jX_i}) = 0$), or by pointing one's main beam to another's side beam ($(M^{I_{MS}}_{X_iX_j} \wedge (D_{X_iX_j} \vee D_{X_jX_i})) = 0$), or by side beam to side beam ($M^{I_{SS}}_{X_iX_j} = 0$). Equations (3.17) and (3.18) can be viewed as the general case of (2.2), while (3.19) can be viewed as the general case of (2.8). Thus, (3.17), (3.18), and (3.19) can be readily applied to many existing analysis methods.

3.2 Minimum Separable Condition in Wireless Multi-Hop Ad Hoc Access Networks

The following derivation shows the application of (3.17)-(3.19) to the wireless ad hoc access networks. The *minimum separable condition* of relay nodes is analytically derived, resulting in the maximum frequency reuse and, hence, the highest capacity.

Consider the scenario as in Figure 3.3(a) where relay nodes are placed within the communication range of a gateway. Suppose that nodes S_1 and S_2 are outside the coverage r

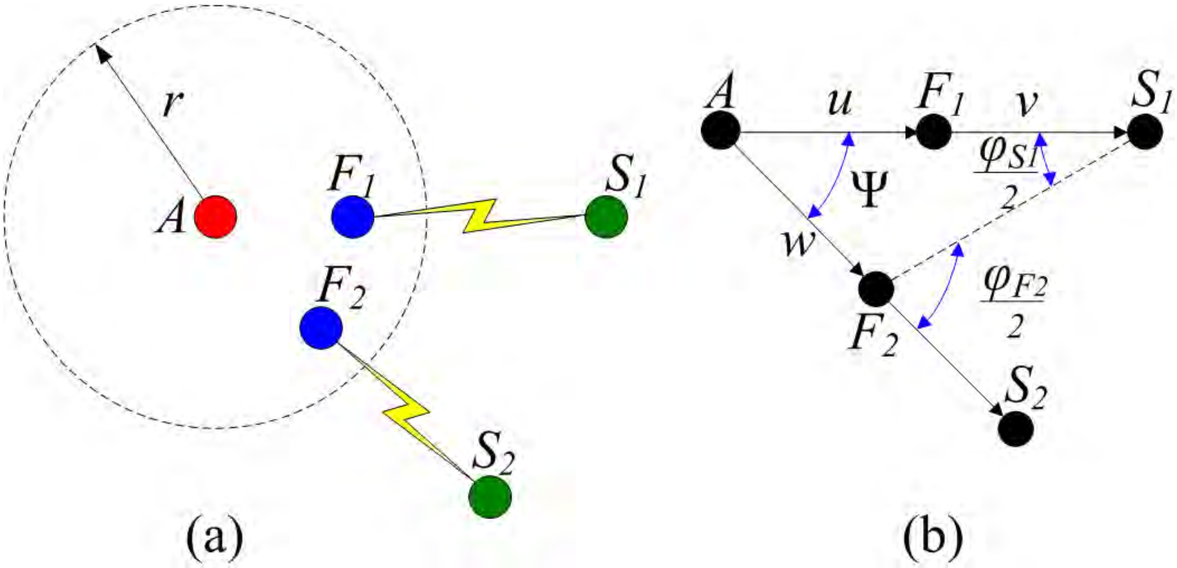

Figure 3.3: Concurrent transmissions in 2-hop relaying wireless ad hoc access networks with directional antenna

of the gateway A and want to connect to the Internet, thus they must connect via relay nodes F_1 and F_2, respectively. Assuming homogeneous perfect steered-beam antenna [32] and symmetrical node placement [14], Figure 3.3(b) shows the vector representation of the scenario, where u, v, w are normalized distances that satisfied (3.17)-(3.18), and φ is antenna beamwidth. The goal is to find the minimum value of Ψ that allows concurrent transmissions of node pairs (F_1, S_1) and (F_2, S_2). This is in fact important because, by allowing concurrent transmissions of all indirect connections, the overall capacity is then bounded by the air-time of gateway, not by other interfering nodes. It can be seen from Figure 3.3(b) that

$$\|\overrightarrow{F_2F_1}\| = \sqrt{w^2 + u^2 - 2wu\cos(\Psi)}, \tag{3.20}$$

$$\|\overrightarrow{F_2S_1}\| = \sqrt{w^2 + (u+v)^2 - 2w(u+v)\cos(\Psi)}. \tag{3.21}$$

For F_1 and F_2 to be interference-free from each other, it all depends on the beamwidth. From (3.19), $M^{I_{MM}}_{F_1F_2}$ must be zero when their main beams can see each other, or $M^{I_{SS}}_{F_1F_2}$ must be zero when the their main beams do not see each other. Due to the assumption of symmetrical node placement, F_1 and F_2 never interfere each other in a main-lobe-to-side-lobe fashion. Moreover, the transmission direction of each node is assumed to be perfect and pointing directly towards the corresponding node. Substituting these conditions by geometrical relationships from Figure 3.3 yield

$$\|\overrightarrow{F_2F_1}\| > \begin{cases} 1+\Delta_{MM}, & \text{if } \frac{\varphi}{2} \geq \cot^{-1}\left[\frac{u\cos(\Psi)-w}{u\sin(\Psi)}\right], \\ 1+\Delta_{SS}, & \text{if } \frac{\varphi}{2} < \cot^{-1}\left[\frac{u\cos(\Psi)-w}{u\sin(\Psi)}\right]. \end{cases} \tag{3.22}$$

The condition of the value of beamwidth in (3.22) is found by varying $\frac{\varphi_{F_2}}{2}$ in Figure 3.3(b) until the dash line intersect F_1. At that point, the main beam of F_2 covers F_1, and vice versa. Similarly, for F_2 and S_1 (or equivalently, F_1 and S_2), to be interference-free from each other, they must satisfy (3.19). Using the same logic in deriving (3.22),

$$\|\overrightarrow{F_2S_1}\| > \begin{cases} 1+\Delta_{MM}, & \text{if } \frac{\varphi}{2} \geq \cot^{-1}\left[\frac{(u+v)\cos(\Psi)-w}{(u+v)\sin(\Psi)}\right], \\ 1+\Delta_{MS}, & \text{if } \cot^{-1}\left[\frac{(u+v)-w\cos(\Psi)}{w\sin(\Psi)}\right] \leq \frac{\varphi}{2} < \cot^{-1}\left[\frac{(u+v)\cos(\Psi)-w}{(u+v)\sin(\Psi)}\right], \\ 1+\Delta_{SS}, & \text{if } \frac{\varphi}{2} < \cot^{-1}\left[\frac{(u+v)-w\cos(\Psi)}{w\sin(\Psi)}\right]. \end{cases} \tag{3.23}$$

The simultaneous communications of node pairs (F_1, S_1) and (F_2, S_2) then must satisfy both (3.22) and (3.23). Note that the conditions for S_1 and S_2 can be neglected, as they are satisfied by the conditions for F_1 and F_2 in this particular type of node placement.

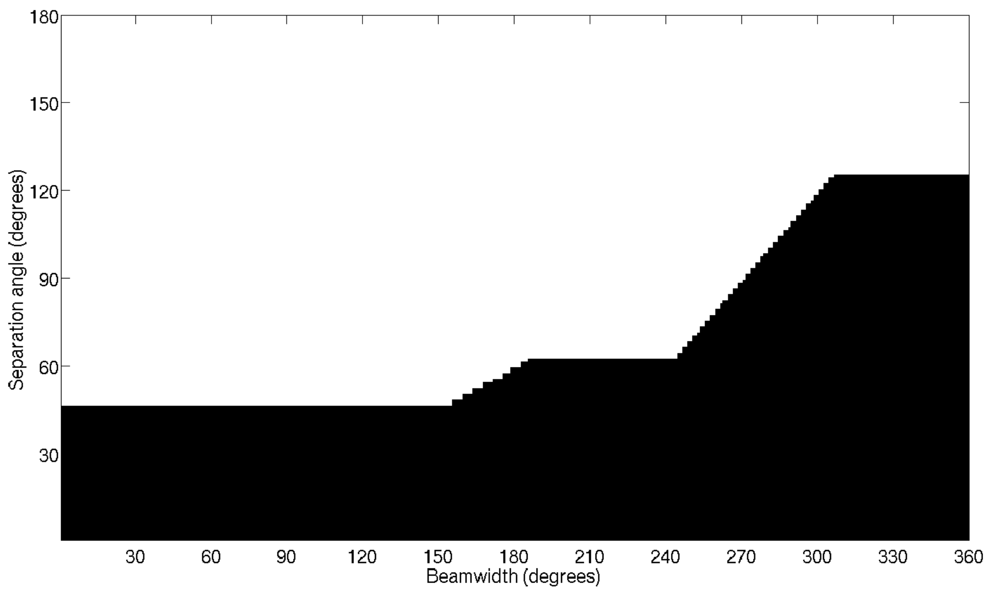

Figure 3.4: Allowable values of separation angle Ψ for any given beamwidth φ with side-beam gain $G_S = 0.2$

By substituting (3.20) into (3.22), and (3.21) into (3.23), the condition for the value of Ψ is obtained. Thus, for any given φ, G_M, and G_S, the minimum separation angle, which is the minimum value of Ψ, and hence the maximum number of simultaneously communicating node pairs, can be found. For instance, if $\xi = 10\text{dB}, G_M = 1, G_S = 0.2, u = v = w = 1$, then the allowable values of Ψ for any given φ are shown in Figure 3.4, where *white* area indicates the non-interfered combination.

Define $\Psi_{\min}(\varphi)$ as the minimum value of Ψ that allows concurrent transmissions for the given φ. Consequently, the maximum number of concurrent pairs can be found from Figure 3.4 by $\lfloor \frac{2\pi}{\Psi_{\min}(\varphi)} \rfloor$, which ranges from 2 (when $\varphi > 300°$) to 7 (when $\varphi < 163°$). An example of effective hybrid antenna pattern for the scenario of Figure 3.3 when $\varphi = 45°$ and $\Psi = \frac{360}{7}°$ is shown in Figure 3.5. Different interference ranges are shown by different shades of colors, similar to Figure 3.2. As long as the corresponding zones of a node do not overlap other nodes (except its communicating node), then it can transmit without interfering other nodes.

In another example, suppose that the side-beam gain G_S changes to 0.1. The smaller side-beam gain results in smaller interference zones. The allowable values of Ψ for any given φ are shown in Figure 3.6, where white area indicates the non-interfered combination. In this case, there could be as many as 11 concurrent transmissions, since $\lfloor \frac{2\pi}{\Psi_{\min}(\varphi)} \rfloor = 11$ at the smallest beamwidth.

The maximum number of concurrent pairs is significant because it is directly related to the capacity of the network [14]. By allowing all pairs to communicate simultaneously, spatial reuse will be fully appreciated, and the overall throughput will not be bounded by the number of nodes. In fact, an optimal scheduling can be obtained when all possible communication pairs can be concurrent pairs. For example, from Figure 3.3(a), suppose that (F_1, S_1) can communicate simultaneously with (F_2, S_2), as well as (F_1, S_1) with (A, F_2), and (A, F_1) with (F_2, S_2), then an optimal scheduling is shown as in Table 3.1 which repeats every 4 slots. It can be seen that all nodes have an equivalent of 1 slot to access the Internet, so, in n-node network, the per-node throughput is $\frac{1}{n}$. Furthermore, the gateway A is always busy, which means the capacity is fully utilized, and the normalized overall capacity is unity.

3.3 Summary

This chapter provides an analytical framework based on the reception conditions for wireless multi-hop ad hoc access networks with directional antenna. The novelty of the proposed formula is in the usage of the vector representations. Furthermore, the conditions

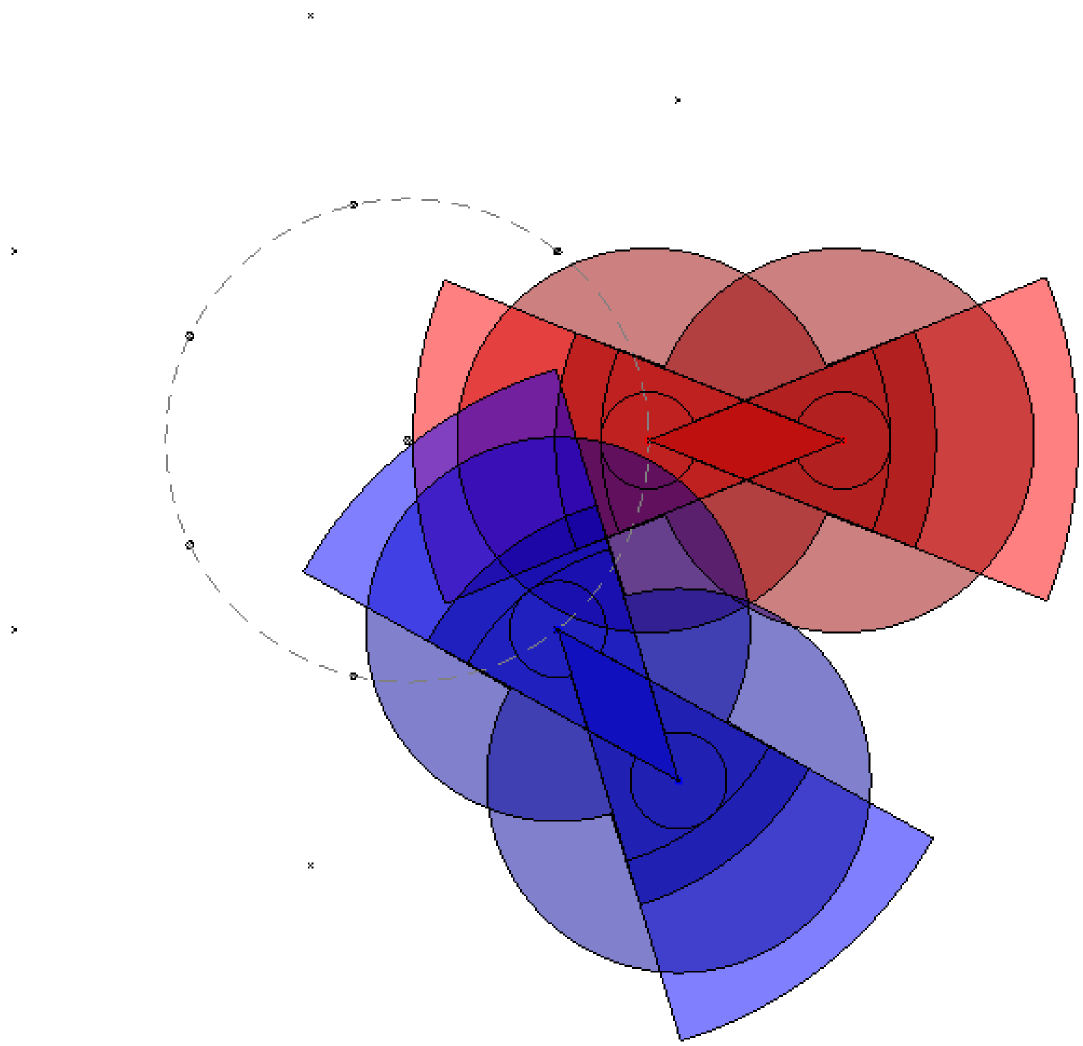

Figure 3.5: Example of effective hybrid antenna pattern for beamwidth $\varphi = 45°$, when separation angle $\Psi = \frac{360}{7}°$

Table 3.1: Possible scheduling for 2-hop relaying wireless ad hoc access networks with directional antenna

Time Slot	Communicating Pairs
Slot1	(A, F_1) for data of S_1
Slot2	(A, F_2) for data of S_2
Slot3	(A, F_1) for data of F_1, and (F_2, S_2) for data of S_2
Slot4	(A, F_2) for data of F_2, and (F_1, S_1) for data of S_1

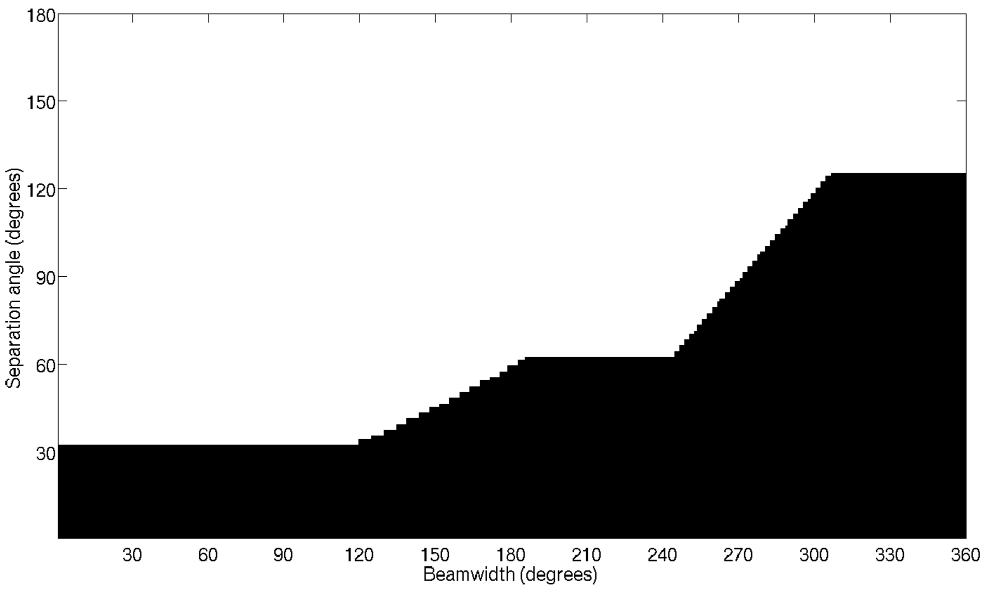

Figure 3.6: Allowable values of separation angle Ψ for any given beamwidth φ with side-beam gain $G_S = 0.1$

for simultaneous communications are neatly formulated as (3.17)-(3.19), avoiding the complicated and often-confusing directional-based protocol constraints. These conditions are applicable to plenty of existing techniques that were intended for omnidirectional antenna only.

One application of the conditions are shown in Section 3.2. The result is meaningfully described as the minimum separable condition for multi-hop ad hoc access networks. Satisfying this condition can guarantee simultaneous transmissions around a gateway. Finding a proper scheduling to fully utilize the gateway becomes easy. However, finding a proper number of hops to reach a distant node is not clearly understood. More specifically, the proper placement of relays that yields the maximum capacity is yet to be discussed. Conventional wisdom often relies on the fewest number of hops by placing relays at the farthest from each other and still maintaining the connectivity. This approach may not be optimal though. The condition of optimal relay placement can be found in Chapter V, using the results from Chapter IV.

CHAPTER IV

SHANNON CAPACITY OF SINGLE HOP COMMUNICATION IN SPATIALLY UNIFORM INTERFERENCE ENVIRONMENT

The result from Chapter III gives insights in relay positioning for a constant data rate between all node-pairs. However, there are other factors that have been ignored that could highly influence the capacity. In this chapter, the concept of reception condition is relaxed. Thus, to find an upper bound of capacity of a node pair equipped with directional antenna, Shannon capacity is utilized. Section 4.1 gives an analysis on the impact of overall interference to the capacity bound of a single-hop communication. The analysis is performed in a general case. Hence, it is applicable to both omnidirectional and directional antenna deployment, given that all nodes are using the same type of antenna. Section 4.2 gives the verification of the analytical result by comparing it with simulations using a realistic antenna pattern. The effects of beamwidth and node activity ratio are also studied. Section 4.3 summarizes the findings in this chapter.

4.1 Analysis of Equivalent Interferers

From (2.9), a reception capacity $C^{\mathbf{T}}_{X_iX_j}$ of a receiver X_j from a transmitter X_i when other nodes $X_k \in \mathbf{T}$, $k \neq i$ are also transmitting is given by

$$C^{\mathbf{T}}_{X_iX_j} = BW \log_2 \left(1 + \frac{\dfrac{H_{X_iX_j} P}{|X_i - X_j|^{\alpha}}}{N + \displaystyle\sum_{k \in \mathbf{T}, k \neq i} \frac{H_{X_kX_j} P}{|X_k - X_j|^{\alpha}}} \right). \tag{4.1}$$

As mentioned in Section 2.2, (4.1) exemplifies that the capacity not only depends on the received power from the intended transmitter, but also suffers from the other transmitters of other communications. Thus, calculating the interference power becomes a key point in the analysis.

Assume that nodes are spatially randomly distributed with node density function $f(r,\theta)$ in polar-coordinated 2-dimensional plane. Then, the interference power I, perceived by a receiver R locating at the origin, can be given by

$$I = \int_{0}^{2\pi} \int_{r_{\min}}^{\infty} \frac{G_R G_I P}{r^{\alpha}} a f(r,\theta)\, r dr d\theta. \tag{4.2}$$

Here, G_R and G_I are the antenna gains of R and interferers, respectively. And a is the interferer node activity ratio, defined as the percentage of nodes that act as transmitters in a given time. This ratio can be viewed as either directly related to the traffic demand, or used as a control parameter in a network. Note the guard zone in (2.5) is represented as the lower limit of integration $r_{\min}$ in (4.2), also called *silent region* [35]. In practice, appropriate setting of $r_{\min}$ has an important implication in protocol design to prohibit potentially interferer nodes from transmitting anything at all. For networks of nodes equipped with omnidirectional antenna, the antenna gain is independent from the node orientation. However, for nodes with directional antenna considered in this dissertation, the gain G_{X_i} follows (2.13). Using this cone-plus-ball antenna model, (4.2) can be written as

$$\begin{aligned} I &= \int_{\theta\in\mathbf{\Gamma}} \int_{r_{MS}}^{\infty} \frac{G_{RM} G_{TS} P}{r^{\alpha}} (1-q)\, a f(r,\theta)\, r dr d\theta \\ &+ \int_{\theta\in\mathbf{\Gamma}} \int_{r_{MM}}^{\infty} \frac{G_{RM} G_{TM} P}{r^{\alpha}} (q)\, a f(r,\theta)\, r dr d\theta \\ &+ \int_{\theta\notin\mathbf{\Gamma}} \int_{r_{SS}}^{\infty} \frac{G_{RS} G_{TS} P}{r^{\alpha}} (1-q)\, a f(r,\theta)\, r dr d\theta \\ &+ \int_{\theta\notin\mathbf{\Gamma}} \int_{r_{SM}}^{\infty} \frac{G_{RS} G_{TM} P}{r^{\alpha}} (q)\, a f(r,\theta)\, r dr d\theta, \end{aligned} \tag{4.3}$$

where $\mathbf{\Gamma}$ denotes the range of angles that the main lobe covers, depending on the beamwidth, and q denotes the proportion of nodes that *point* their main lobes to the origin (or any point in general). Assuming that transmission direction is random with uniform distribution, then

$$q = \frac{\varphi}{2\pi}, \tag{4.4}$$

$$\int_{\theta\in\mathbf{\Gamma}} d\theta = 2\pi q. \tag{4.5}$$

In (4.3), note that the additional subscripts T and R of antenna gains are used to specify the gains of transmitter and receiver, respectively, purposefully for the clarity of the derivation. This work assumes that $G_{RM} = G_{TM} = G_M$ and $G_{RS} = G_{TS} = G_S$. The usage of different lower limits in (4.3) for each integral can also be found in [40]. While [40] concentrates on effects of variations of lower limits, this dissertation assumes them to be adjustable protocol parameters. For a general case of uniform node distribution, or, equivalently, the homogeneous Poisson point process of node location, with node density D (nodes/unit area),

$$f(r,\theta) = D. \tag{4.6}$$

Then, (4.3) can be written as

$$I = \frac{2\pi a P D}{\alpha - 2}\left(\frac{G_{RM}G_{TS}q(1-q)r_{MS}^2}{r_{MS}^\alpha} + \frac{G_{RM}G_{TM}q^2 r_{MM}^2}{r_{MM}^\alpha} + \frac{G_{RS}G_{TS}(1-q)^2 r_{SS}^2}{r_{SS}^\alpha} + \frac{G_{RS}G_{TM}(1-q)q r_{SM}^2}{r_{SM}^\alpha}\right). \tag{4.7}$$

Define

$$\begin{aligned} F_{RM} &= qG_{RM}, \\ F_{TM} &= qG_{TM}, \\ F_{RS} &= (1-q)G_{RS}, \\ F_{TS} &= (1-q)G_{TS}, \end{aligned} \tag{4.8}$$

as the *equivalent* gains. Substituting (4.8) to (4.7) yields

$$I = \frac{2\pi a P D}{\alpha - 2}\left(\frac{F_{RM}F_{TS}r_{MS}^2}{r_{MS}^\alpha} + \frac{F_{RM}F_{TM}r_{MM}^2}{r_{MM}^\alpha} + \frac{F_{RS}F_{TS}r_{SS}^2}{r_{SS}^\alpha} + \frac{F_{RS}F_{TM}r_{SM}^2}{r_{SM}^\alpha}\right). \tag{4.9}$$

Since the form of (4.9) mimics the general path-loss equation, one can view (4.9) as the equivalence of having 4 distinct interferers, similar to the concept of center of mass. Each equivalent interferer is placed at the boundaries of the allowed regions and has distinct transmitted power and gain. Figure 4.1 shows an illustration of the equivalent interferers. Note that (4.9) is the average interference power for any receiver under the homogeneous environment. Specifically, in this model, each node is randomly placed with the same node density, is being active randomly, and transmits to a random angle. In practice, a node-pair naturally does not exclusively communicate continuously, but transmits to various nodes

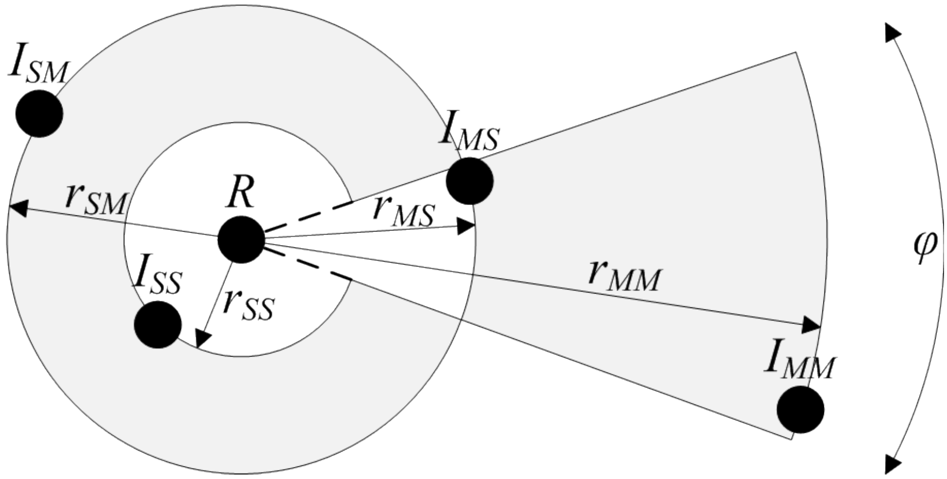

Figure 4.1 Equivalent interferers

depending on traffic demand. Thus, on the long run average, the node's activity is similar to the model, and the expected interference power equals to (4.9), which directly influents the expected throughput. This allows simple calculations of capacity bound of a wireless network equipped with directional antenna. Using (4.9) for a homogeneous environment, the interference term in (4.1) can then be rewritten, and the reception capacity $C_{X_iX_j}$ is expressible as

$$C_{X_iX_j} = BW \log_2 \left(1 + \frac{\frac{G_{RM}G_{TM}P}{|X_i - X_j|^{\alpha}}}{N + \frac{2\pi aPD}{\alpha - 2}\left(\frac{F_{RM}F_{TS}}{r_{MS}^{\alpha-2}} + \frac{F_{RM}F_{TM}}{r_{MM}^{\alpha-2}} + \frac{F_{RS}F_{TS}}{r_{SS}^{\alpha-2}} + \frac{F_{RS}F_{TM}}{r_{SM}^{\alpha-2}}\right)} \right), \tag{4.10}$$

for any active pair (X_i, X_j) that point their main beams to each other for the best reception.

The applicability of (4.9) is not only for network with the steered-beam antenna, but also for network with simple switched-beam antenna. While the common deployment of the switched-beam antenna is done by activating a single beam at a time, one can also view the activation of multiple consecutive beams as effectively widening the beamwidth. Figure 4.2(a) shows 2 consecutive beams of the 8-element UCA antenna patterns that are $30°$ apart. Figure 4.2(b) shows the combined antenna pattern of the 2 beams. Figure 4.3 and Figure 4.4 give the beam patterns of 1 to 12 consecutive 8-element UCA beams being turned on counterclockwise. Increasing beamwidth in this fashion means reducing the accuracy needed in estimating the location of the intended destination. That said, there must be a tradeoff in terms of capacity and this tradeoff must be investigated.

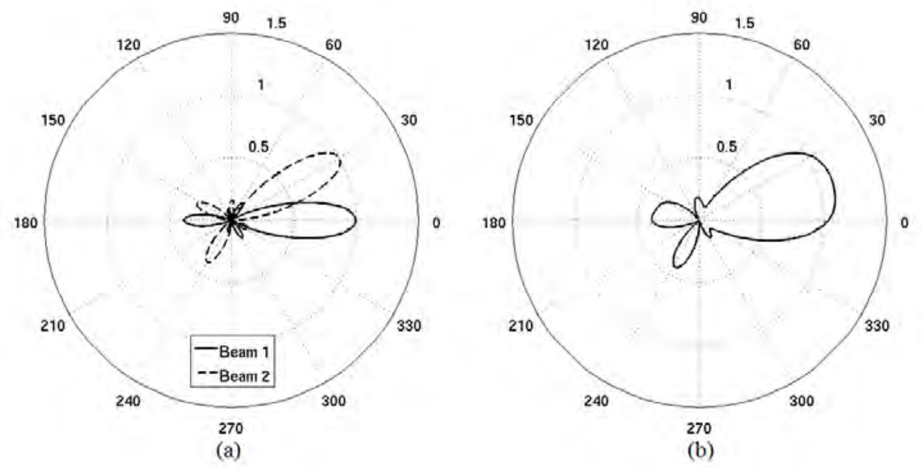

Figure 4.2 Wider beamwidth resulting from switching-on multiple beams

With the multi-beam scheme, the set of active beam angles $\theta(\psi_{X_i})$ is redefined as

$$\begin{aligned} \theta(\psi_{X_i}) = \left\{\theta : \phi_{X_i} + \psi_{X_i} - \frac{b\varphi}{2} \le \theta \le \phi_{X_i} + \psi_{X_i} + \frac{b\varphi}{2}\right\}, \\ \psi_{X_i} \in \left\{0, \frac{2\pi}{B}, \frac{4\pi}{B}, \dots, \frac{2(B-1)\pi}{B}\right\}, \end{aligned} \tag{4.11}$$

where b is the number of switched-on beams. The value of the cone-plus-ball antenna gains become

$$G_{X_i}(\theta) = \begin{cases} G_M + (n-1)G_S, & \text{if } \theta \in \theta(\psi_{X_i}), \\ nG_S, & \text{otherwise.} \end{cases} \tag{4.12}$$

The value of F_{RM}, F_{TM}, F_{RS} and F_{TS} for a network with switched-beam antenna then can be given by

$$\begin{aligned} F_{RM} &= F_{TM} = q\left(G_M + (n-1)G_S\right), \\ F_{RS} &= F_{TS} = (1-q)\, nG_S. \end{aligned} \tag{4.13}$$

The effect of widened-combined main beam is captured by q, and the consequence of extra side lobe is shown as $(n-1)G_S$.

4.2 Effects of Activity Ratio and Beamwidth

The factors that affect the reception capacity, as shown in (4.10), besides the distance between the node pair, are the node activity ratio and antenna-related parameters. Particu-

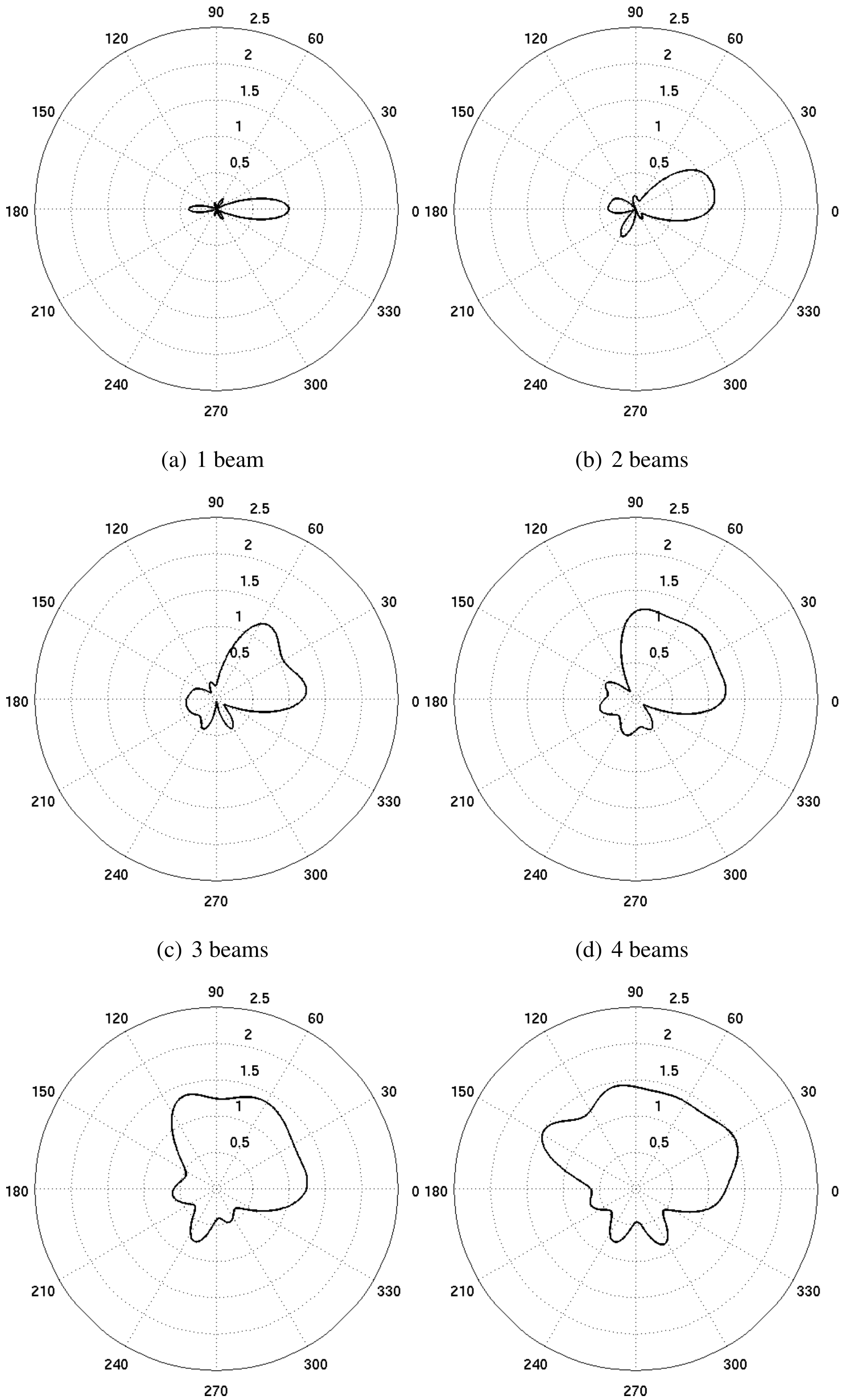

(a) 1 beam
(b) 2 beams
(c) 3 beams
(d) 4 beams
(e) 5 beams
(f) 6 beams

Figure 4.3 Antenna pattern of 1 to 6 consecutive 8-element UCA beams

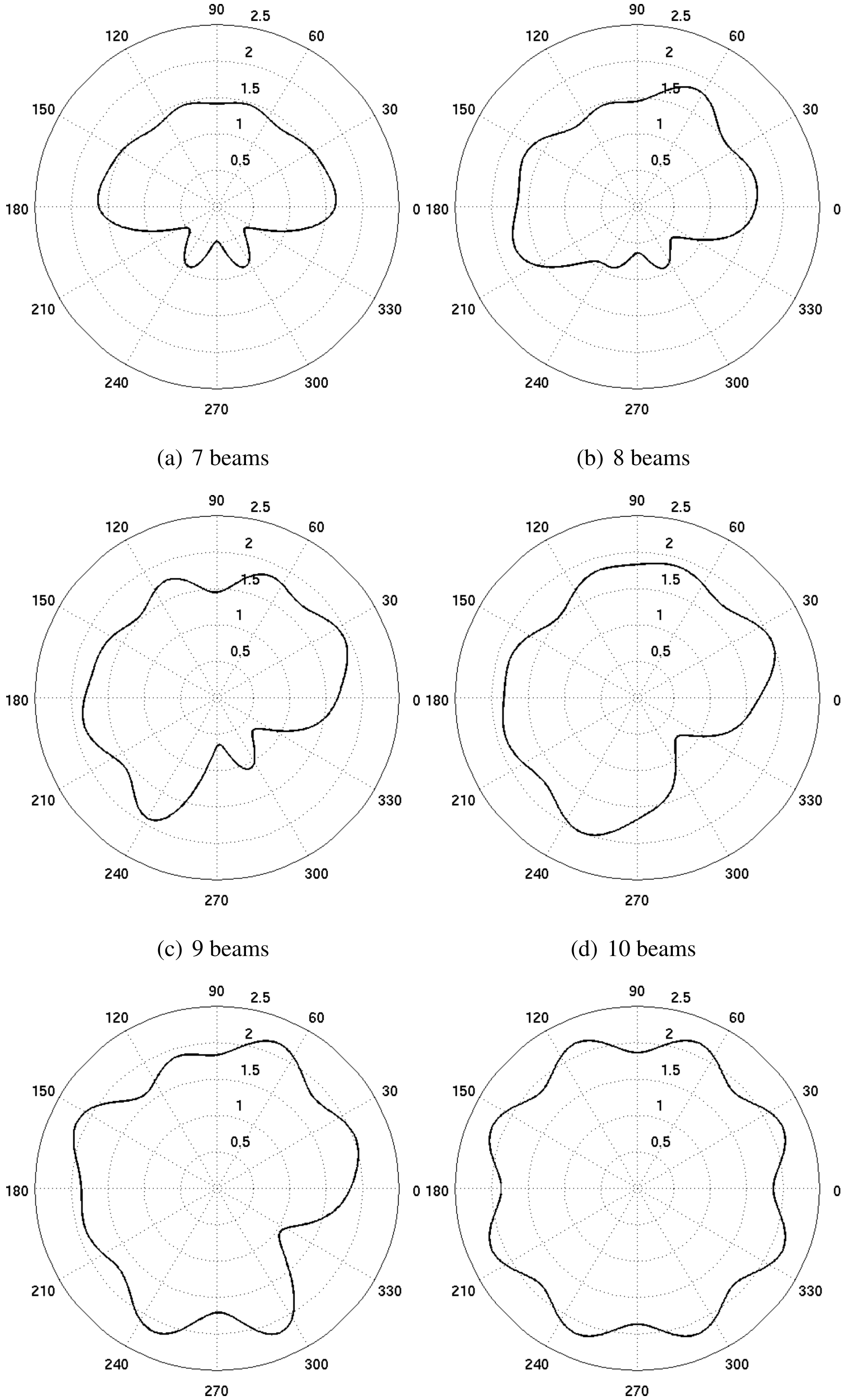

(a) 7 beams (b) 8 beams

(c) 9 beams (d) 10 beams

(e) 11 beams (f) 12 beams

Figure 4.4 Antenna pattern of 7 to 12 consecutive 8-element UCA beams larly, the effects of node activity ratio a and antenna beamwidth φ are shown in this section. While using the cone-plus-ball antenna model yields tractable analysis, the results must be compared with a realistic antenna model to confirm its usefulness. For this purpose, the 8-element uniform circular array (UCA) [39] is here used for comparison with the derived formula. Their beam patterns are shown in Figure 4.3 and Figure 4.4. Verification is done via simulations using Monte Carlo method. Node locations are uniformly randomly distributed in a circular area with diameter of 400 m. The total interference power received at the origin from 1000 realizations for each specific input is calculated for the mean value and its 95% confidence interval, and compared with the analytical results using the cone-plus-ball model. The parameter settings are $\alpha = 4$, $BW = 1$ Hz, $P = 1$ W, $N = 0$ (negligible in comparison with the resultant interference), $|X_i - X_j| = 1$ m, and $D = 1\ \text{Node}/\text{m}^2$. All of these are normalized for simple adaptation. The directional antenna-related settings are $G_M = 1$, $G_S = 0.12$, $r_{MM} = 10\sqrt{10}$ m, $r_{MS} = r_{SM} = 10$ m, and $r_{SS} = \sqrt{10}$ m.

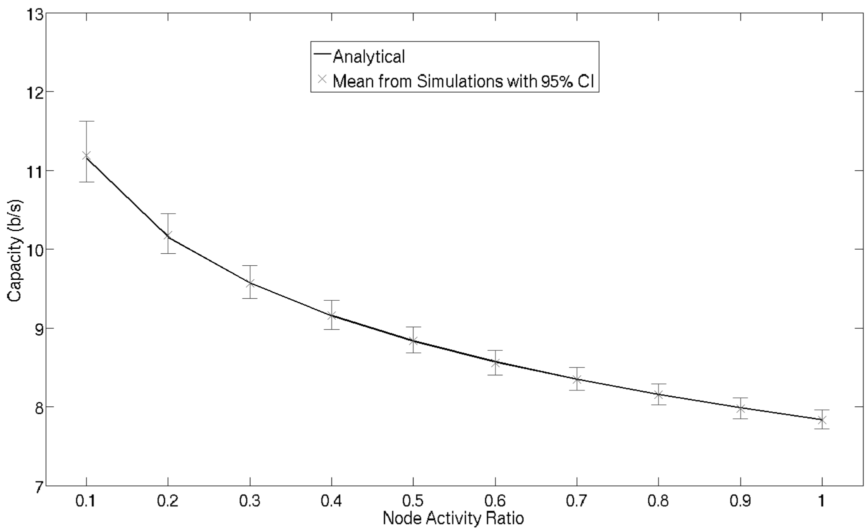

Figure 4.5: Analytical results compared with means and 95% confidence intervals from simulations of capacity at various node activity ratio

To find the effect of node activity ratio, each active node X_k is equipped with 8-element UCA steered-beam antenna with uniformly distributed random orientation ϕ_{X_k} and transmission direction ψ_{X_k} which emits power as if transmitting to a receiver. Note that some node is not allowed to transmit if it falls in a prohibited area around the origin, the location of the receiver of interest which has a directional antenna points towards a random angle. The result of the capacity derived from (4.1) is shown in Figure 4.5. As expected, the capacity drops when the activity ratio increases. This shows the impact of the interference from other concurrent transmissions. This fact is normally hidden in the common Protocol Model. Therefore, the tradeoff must be carefully studied, as higher capacity per pair means fewer concurrent transmissions. For the verification purpose, the mean values from the simulations match closely with the analytical results. This confirms the validity of the cone-plus-ball model and the analysis itself.

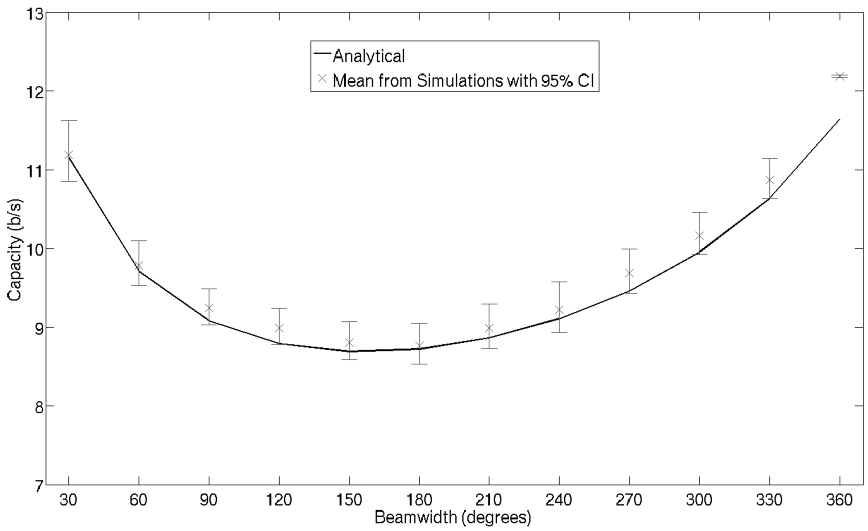

Figure 4.6: Analytical results compared with means and 95% confidence intervals from simulations of capacity at various beamwidth

To observe the effect of beamwidth, the switched beam antenna is considered for its simplicity in varying the beamwidth for UCA. The 8-element UCA with random orientation ϕ_{X_k} and transmission direction ψ_{X_k} is applied, but to achieve the effect of switched-beam beamwidth variation, b consecutive beams are turned on so the effective beamwidth $\varphi = b \times 30°$, for $b = 1$ to 12. Interestingly, $b = 12$ is the equivalence of omnidirectional antenna. Thus, a direct comparison can be made to show the effectiveness of directionality. Without loss of generality, the result of the capacity derived from (4.1) is shown in Figure 4.6 for $a = 0.1$. The mean values from the simulations again are agreed with the analytical results, although some deviation existed at large beamwidth, which caused by accumulated errors of the cone-plus-ball antenna model compared to the UCA. It also shows that capacity is the highest at the equivalence of omnidirectional antenna, resulting from the largest silent region. However, it implies that more nodes are suppressed from transmissions, and the *actual* activity ratio is lower than the preset value. Ultimately, the capacity *per area* is reduced. This effect must be carefully observed, and a special case is discussed in Chapter V.

4.3 Summary

In this chapter, the reception conditions from Chapter III are relaxed and concentration is on the maximum-possible capacity. Random node placements with uniform node density is applied as interferers from a point of view of a node. Those interferers can be collectively viewed as equivalent interferers. Shannon capacity of a node from a single hop transmission is then analytically derived. The analytical result is also numerically compared to Monte Carlo simulations of realistic antenna patterns, which shows good agreements. The flexibility of the formulation in this chapter also opens the door for the analysis of multi-hop transmissions, to be found in the next chapter.

CHAPTER V

OPTIMAL CAPACITY OF MULTI-HOP AD HOC ACCESS NETWORKS

The aforementioned capacity derived in Section 4.1 is for a direct transmission of a node-pair in a uniform interference environment. However, that capacity decays quickly with the distance between the node-pair, as shown in (4.10). To overcome such problem, networks commonly rely on multi-hop relaying. Nevertheless, the analysis of multi-hop network capacity in the literature normally involves either the limit of reception conditions [5] or the scheduling policy [14]. Protocols that govern multi-hop transmissions become complex and difficult to analyze too. This chapter proposes an extension of the framework from Chapter IV to deal with the multi-hop transmission scenario. Capacity bound derived in this chapter is protocol-independent. In the following, Section 5.1 shows the derivation of a special case of 1-dimensional network and its capacity bound. The multi-hop capacity is provided in Section 5.2. Section 5.3 gives the improvement of the directional-antenna-equipped network capacity in comparison with the omnidirectional one. The chapter's final remarks are given in Section 5.4.

5.1 Capacity Bound of 1-Dimensional Networks

The aim of this chapter is to find the optimal capacity from a source to a destination through a possibility of relaying. The environment considered here is similar to what appeared in Chapter IV, except that the node-location space is simplified from 2 dimensions to 1 dimension. The results and insights gained from this simplified model can be applied to the more general cases in the future investigations. Also, a 1-dimensional network can be viewed as a simplified model of each *branch* of the network in Section 3.2.

Since the node location space of consideration becomes 1-dimensional, the derivation in Section 4.1 must be modified. Assume that nodes are randomly distributed with node density function $f(r)$ on a line. Furthermore, assume that the environment is homogeneous,

$f(r) = D$. The equivalence of (4.2) for 1-dimensional network is

$$I = \int_{-\infty}^{-l_{\min}} \frac{G_R G_I P}{r^{\alpha}} aDdr + \int_{r_{\min}}^{\infty} \frac{G_R G_I P}{r^{\alpha}} aDdr, \tag{5.1}$$

where the value of $l_{\min}$, $r_{\min}$ depends on protocol parameter settings and antenna directions. Assume that all nodes have the same alignment, $\phi_{X_i} = 0,\ \forall X_i$, the antenna direction ψ_{X_i} can be given by

$$\psi_{X_i} = \begin{cases} 0, & \text{when it points to the right,} \\ \pi, & \text{when it points to the left.} \end{cases} \tag{5.2}$$

Then, the equivalence of (4.3) for 1-dimensional network is

$$\begin{aligned} I = &\int_{r_{MS}}^{\infty} \frac{G_{RM} G_{TS} P}{r^{\alpha}} (1-q)\, aDdr + \int_{r_{MM}}^{\infty} \frac{G_{RM} G_{TM} P}{r^{\alpha}} (q)\, aDdr \\ &+ \int_{r_{SS}}^{\infty} \frac{G_{RS} G_{TS} P}{r^{\alpha}} (1-q)\, aDdr + \int_{r_{SM}}^{\infty} \frac{G_{RS} G_{TM} P}{r^{\alpha}} (q)\, aDdr, \end{aligned} \tag{5.3}$$

where q denotes the proportion of nodes that point their main lobes to the origin. Performing integrations in (5.3) yields

$$\begin{aligned} I = \frac{aPD}{\alpha - 1} \Bigg(&\frac{G_{RM} G_{TS} (1-q) r_{MS}}{r_{MS}^{\alpha}} + \frac{G_{RM} G_{TM} q r_{MM}}{r_{MM}^{\alpha}} \\ &+ \frac{G_{RS} G_{TS} (1-q) r_{SS}}{r_{SS}^{\alpha}} + \frac{G_{RS} G_{TM} q r_{SM}}{r_{SM}^{\alpha}} \Bigg). \end{aligned} \tag{5.4}$$

The result is again in the form of equivalent interferers. Consequently, for any active pair (X_i, X_j) that point their main beams to each other for the best reception, the Shannon capacity $C(\mathcal{R})$ for $\mathcal{R} = |X_i - X_j|$ is given by

$$C(\mathcal{R}) = BW \log_2 \left(1 + \frac{\frac{G_{RM} G_{TM} P}{\mathcal{R}^{\alpha}}}{N + \frac{aPD}{\alpha-1} \left(\frac{(1-q) G_{RM} G_{TS}}{r_{MS}^{\alpha-1}} + \frac{q G_{RM} G_{TM}}{r_{MM}^{\alpha-1}} + \frac{(1-q) G_{RS} G_{TS}}{r_{SS}^{\alpha-1}} + \frac{q G_{RS} G_{TM}}{r_{SM}^{\alpha-1}} \right)} \right). \tag{5.5}$$

This result is going to be used in the derivation for multi-hop transmissions in 1-dimensional networks. Since the concentration is on the effect of interferers, assume that N is negligible in comparison with the resultant interference. Furthermore, define

$$K = \frac{(\alpha-1)G_{RM}G_{TM}}{(1-q)\frac{G_{RM}G_{TS}}{r_{MS}^{\alpha-1}} + q\frac{G_{RM}G_{TM}}{r_{MM}^{\alpha-1}} + (1-q)\frac{G_{RS}G_{TS}}{r_{SS}^{\alpha-1}} + q\frac{G_{RS}G_{TM}}{r_{SM}^{\alpha-1}}}. \tag{5.6}$$

Note that K is a function of antenna gains, silent regions, loss exponent, and proportion of antenna direction. Then (5.5) becomes

$$C(\mathcal{R}) = BW\log_2\left(1 + \frac{K}{aD\mathcal{R}^{\alpha}}\right). \tag{5.7}$$

Equation (5.7) gives a capacity bound of communicating nodes with distance $\mathcal{R}$. As the distance increases, especially at $\alpha > 2$, the capacity decreases rapidly. This gives a motivation in utilizing multi-hop relaying.

5.2 Multi-Hop Relaying and Optimal Capacity

In multi-hop relaying scenarios, nodes must add the network layer functionality into the operation. Thus, the media access control is evolved into scheduling policies. In finding a bound, however, the perfect scheduling that maximizes the capacity is assumed. In other words, the overhead time of media access is neglected. Each node can transmit when it is not prohibited by other nodes and the intended receiver is available.

The concept of end-to-end capacity through relaying can be illustrated by the following example. Suppose that there are 3 nodes placed on a line as in Figure 5.1, and X_i wants to send b bits of data to X_j by using 2-hop transmissions via X_r. Define C_1 as a capacity of transmission from X_i to X_r, and C_2 as a capacity of transmission from X_r to X_j. Thus, the transmission time t_1, t_2 used in transmitting b bits through capacity C_1, C_2, respectively, are given by

$$t_1 = \frac{b}{C_1}, t_2 = \frac{b}{C_2}. \tag{5.8}$$

Figure 5.1 Example of scenario in multi-hop relaying

The total time t to convey b bits from X_i to X_j is

$$t = t_1 + t_2 = \frac{b}{C_1} + \frac{b}{C_2}. \tag{5.9}$$

Hence, the end-to-end capacity C_{e2e} [41], defined as the number of bits that can be conveyed per unit time, is given by

$$C_{e2e} = \frac{b}{t} = \frac{1}{\dfrac{1}{C_1} + \dfrac{1}{C_2}}. \tag{5.10}$$

Equation (5.10) can also be viewed as the analogy of the capacitance of 2 cascading capacitors. The same logic of (5.10) can be applied for more hops of relaying. For $\mathcal{N}$-hop relaying [42], C_{e2e} can be given by,

$$C_{e2e} = \frac{1}{\sum\limits_{k=1}^{\mathcal{N}} \dfrac{1}{C_k}} = \frac{1}{\mathcal{N}} mean_h(C_k), \tag{5.11}$$

where C_k is the capacity of hop k. The operator $mean_h(.)$ refers to the *harmonic mean*. The key property of the harmonic mean is

$$mean_h(C_k) \leq mean(C_k), \tag{5.12}$$

where the operator $mean(.)$ is the arithmetic mean. The two means in (5.12) can be equal only when $C_k = C^*, \ \forall k$. In other words, the end-to-end multi-hop capacity is maximized when the capacity of each hop is the same. Using this principle, the maximum $\mathcal{N}$-hop end-to-end capacity C^*_{e2e} is given by

$$C^*_{e2e} = \frac{C^*}{\mathcal{N}}, \tag{5.13}$$

when C^* is the capacity of each hop that must be the same for every hop. Recall that (5.7) is a single-hop capacity, and is applicable to be used as C^*. To reach the distance $\mathcal{R}$ in $\mathcal{N}$ hops, each hop must cover the distance $\frac{\mathcal{R}}{\mathcal{N}}$ equally, i.e.,

$$C^* = C\left(\frac{\mathcal{R}}{\mathcal{N}}\right) = BW \log_2 \left[1 + \frac{K}{aD}\left(\frac{\mathcal{N}}{\mathcal{R}}\right)^{\alpha}\right]. \tag{5.14}$$

Hence, for a transmission of distance $\mathcal{R}$ using $\mathcal{N}$-hop transmission,

$$C^*_{e2e}(\mathcal{R},\mathcal{N}) = \frac{BW}{\mathcal{N}} \log_2 \left[1 + \frac{K}{aD}\left(\frac{\mathcal{N}}{\mathcal{R}}\right)^{\alpha}\right]. \tag{5.15}$$

Equation (5.15) gives a maximum value of end-to-end capacity for a given number of hops $\mathcal{N}$. To find the optimal number of hops that gives the highest bound, one must find the value of $\mathcal{N}$ that satisfies

$$\frac{\partial C^*_{e2e}(\mathcal{R},\mathcal{N})}{\partial \mathcal{N}} = 0. \tag{5.16}$$

The partial derivative of (5.15) with respect to $\mathcal{N}$ can be expressed as

$$\frac{\partial C^*_{e2e}(\mathcal{R},\mathcal{N})}{\partial \mathcal{N}} = \frac{BW}{\mathcal{N}^2 \ln 2}\left(\frac{\alpha \frac{K}{aD}\left(\frac{\mathcal{N}}{\mathcal{R}}\right)^{\alpha}}{1+\frac{K}{aD}\left(\frac{\mathcal{N}}{\mathcal{R}}\right)^{\alpha}} - \ln\left[1+\frac{K}{aD}\left(\frac{\mathcal{N}}{\mathcal{R}}\right)^{\alpha}\right]\right). \tag{5.17}$$

Substitute (5.17) into (5.16) means solving

$$\frac{\alpha \frac{K}{aD}\left(\frac{\mathcal{N}}{\mathcal{R}}\right)^{\alpha}}{1+\frac{K}{aD}\left(\frac{\mathcal{N}}{\mathcal{R}}\right)^{\alpha}} = \ln\left[1+\frac{K}{aD}\left(\frac{\mathcal{N}}{\mathcal{R}}\right)^{\alpha}\right]. \tag{5.18}$$

The solution of (5.18) can be shown as

$$\left[\frac{K}{aD}\left(\frac{\mathcal{N}}{\mathcal{R}}\right)^{\alpha}\right] = e^{W\left(-\frac{\alpha}{e^{\alpha}}\right)+\alpha} - 1, \tag{5.19}$$

where $W(.)$ is the Lambert W function, also known as the product logarithm.

The optimal value of $\mathcal{N}$, denoted by $\mathcal{N}^*$, can then be written as

$$\mathcal{N}^* = \mathcal{R}\left[\frac{aD}{K}\left(e^{W\left(-\frac{\alpha}{e^{\alpha}}\right)+\alpha} - 1\right)\right]^{\frac{1}{\alpha}}. \tag{5.20}$$

More importantly, recall that the left side of (5.19) is in fact the signal-to-interference ratio of each hop in relaying. The right side of (5.19) is a function of the loss exponent α, depending on the environment and normally uncontrollable. The solution reveals that the maximum end-to-end capacity can be achieved by *selecting* relays so that the *SIR* of each hop satisfies (5.19). Surprisingly, it is independent of the distance to reach an actual destination. Furthermore, since the optimal *SIR* is the function of α only, it is applicable to networks with any kind of antenna. Thus, (5.19) gives a practical guideline in selecting relays, and the selections are valid for any destination. This has a strong implication to routing protocols in selecting the next-hop forwarder that maximizes the end-to-end capacity. Figure 5.2 gives the numerical results of (5.19) for a practical range of the value of α.

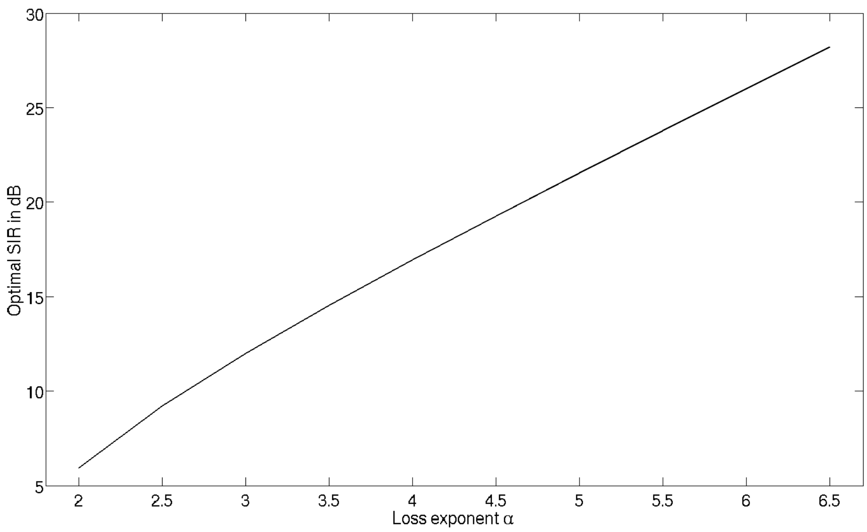

Figure 5.2 Optimal *SIR* as a function of α

5.3 Optimal Capacity of Networks using Omnidirectional and Directional Antenna

To illustrate the effectiveness of multi-hop relaying in terms of capacity, numerical results are shown in this section. Uniformly randomly distributed node locations on a line are assumed. The parameter settings are $BW = 1$ Hz, $P = 1$ W, $N = 0$ (negligible in comparison with the resultant interference), and $D = 1$ Node/m^2. The directional antenna-related settings are $\varphi = 30°$, $G_M = 1$, $G_S = 0.12$, $r_{MM} = 10\sqrt{10}$ m, $r_{MS} = r_{SM} = 10$ m, and $r_{SS} = \sqrt{10}$ m. All of them are carried over from the previous chapter. Furthermore, assume that $q = 0.5$. The reason is, since the network is 1-dimensional, and ψ can only be either 0 or π, then pointing left and right should be equally likely to occur. Since the optimal *SIR* is a function of α, the results are shown as the maximum multi-hop capacity as α is varied. The other factor, as also shown in Section 4.2, is node activity ratio a.

At $\mathcal{R} = 100$ m and $\alpha = 4$, Figure 5.3 shows the numerical results of (5.15) when $\mathcal{N}$ equals (5.20) at various values of a. As a comparison, a direct transmission over distance $\mathcal{R}$ with the same settings is shown in Figure 5.4. The trend of the decaying capacity when increasing a is similar to Figure 4.5. When comparing Figure 5.3 to Figure 5.4, however, the benefit of multi-hops becomes obvious, as the improvement is as large as 3 orders of magnitude.

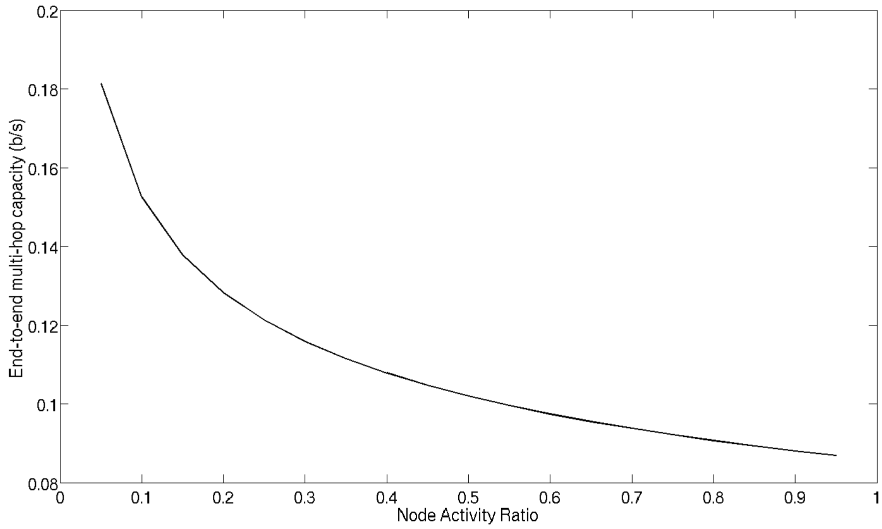

Figure 5.3 Optimal multi-hop capacity as a function of a at $\alpha = 4$ when $\mathcal{R} = 100$m

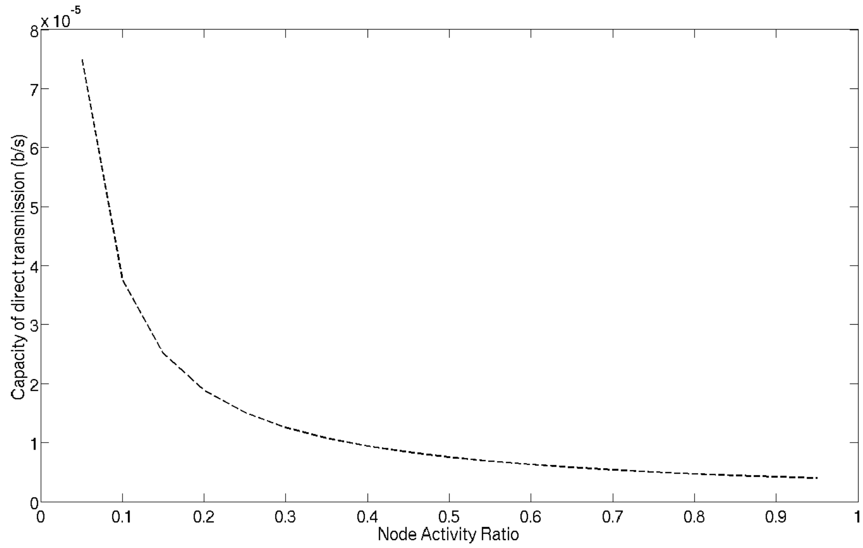

Figure 5.4 Capacity of direct transmission as a function of a at $\alpha = 4$ when $\mathcal{R} = 100$m

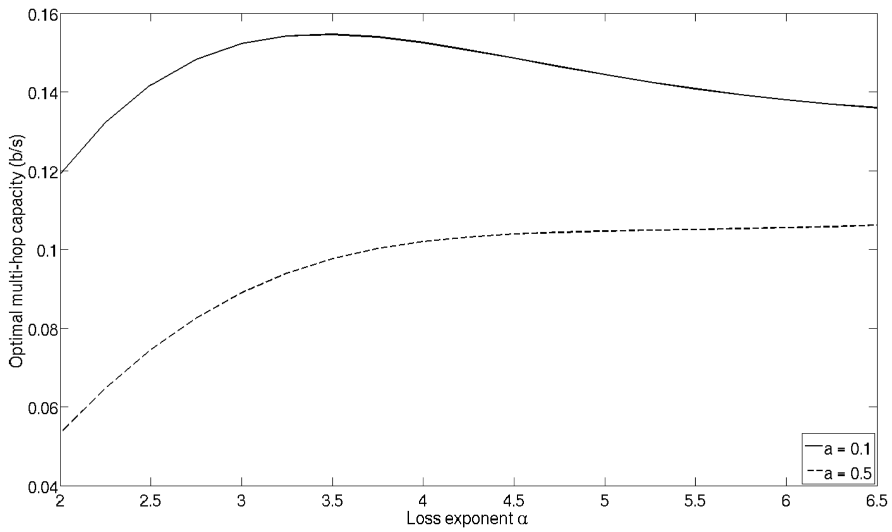

Figure 5.5 Optimal multi-hop capacity as a function of α at $a = 0.1$

The effect of α is shown in Figure 5.5 for $a = 0.1$ and $a = 0.5$ when $\mathcal{R} = 100$ m. The range of α in the plot is selected based on the range of practical values. Interestingly, the low loss exponent α that allows signals to travel farther has a negative effect on the optimal capacity, especially at high interference level caused by high a. At lower interference level, the high loss exponent α takes the toll on intended signal more than the interference, resulting in the decaying of capacity.

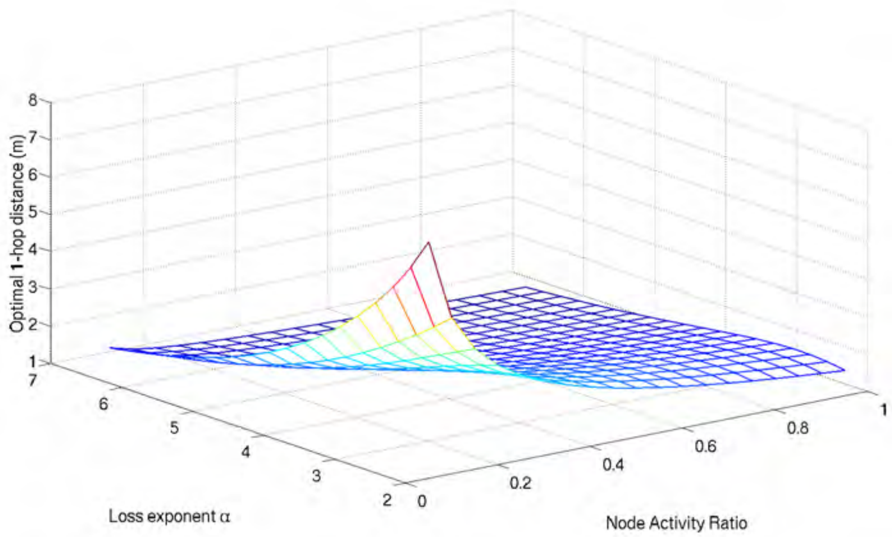

Figure 5.6 Optimal 1-hop distance as a function of a and α

Another interesting result can be found in terms of the optimal *1-hop distance*, defined as the distance between each relay so the resultant *SIR* satisfies (5.19). In other words, it is $\mathcal{R}/\mathcal{N}^*$. Figure 5.6 shows the optimal 1-hop distance as a function of both a and α. Note that this is independent of $\mathcal{R}$. The optimal 1-hop distance is close to 1 in cases that the *SIR* drop quickly with the distance. They are caused by either the high loss exponent α, or the high interference level a. Note that the distance of 1 is the *reference* distance of the propagation model. The propagation model is not valid for the distance less than 1, as it makes the received power greater than the transmitted power, which is not possible.

Finally, to explicitly show the benefit of using directional antenna over the omnidirectional antenna, the comparison must be made. Since the optimal capacity can be met by selecting relays that satisfy (5.19), assume that those relays can be found. Thus, the capacity for each hop is given by (5.14). This means that for the optimal placement, each transmission of each hop has the same capacity, regardless of the antenna type. Therefore, the benefit of using the directional antenna solely lies on the frequency reuse factor. In other words, if a network with directional antenna allows more simultaneous transmissions than a network with omnidirectional antenna, then the capacity per area of the network with directional antenna will be higher. The keyword is *allow*, as it is directly related to the silent region. The question is how many transmitters, or equivalently, how many receivers can be active at a time per distance.

At asymptote, where all nodes attempt to transmit, the number of active nodes per distance is given by the reciprocal of distance that an active node occupies (and prevents other nodes from transmissions). Thus, for a_o, defined as the node activity ratio for networks equipped with omnidirectional antenna,

$$a_o = \frac{1}{2r_{MM}}. \tag{5.21}$$

Similarly, for a_d, defined as the node activity ratio for networks equipped with directional antenna,

$$a_d = \frac{1}{(1-q)r_{MS} + qr_{MM} + (1-q)r_{SS} + qr_{SM}}. \tag{5.22}$$

Hence, the frequency reuse factor is written as

$$\frac{a_d}{a_o} = \frac{2r_{MM}}{(1-q)r_{MS} + qr_{MM} + (1-q)r_{SS} + qr_{SM}}. \tag{5.23}$$

Since $r_{MM} \geq r_{MS} \geq r_{SM} \geq r_{SS}$, networks with directional antenna can always have more concurrent transmissions, and higher overall capacity.

5.4 Summary

In this chapter, Shannon capacity for single-hop transmissions is extended. Based on the homogeneous assumptions of random node placement, node activity, and transmission direction, the multi-hop capacity bound of 1-dimensional networks is analytically derived. With homogeneous assumptions, the capacity bound can be achieved by selecting proper intermediate nodes as relays. The criterion for selecting the best relay of each hop is simply based on the optimal *SIR* for a particular environment. A node that has the closest *SIR* level to the optimal value should be selected as a relay. Each relay node then must select another node that is closer to the destination and has the proper *SIR* level as the next hop relay. The optimal 1-hop distance that yields the optimal *SIR* level is illustrated.

The resultant multi-hop capacity bound is then expressed numerically against various settings. The effects of node activity ratio and loss exponent of the environment are shown. Finally, the benefit of using directional antenna is expressed. The comparison is possible only when each individual transmission has the same capacity, regardless of antenna type. Without the finding of the optimal *SIR*, different type of antenna cannot be compared straightforwardly.

One can view the result from this chapter as a complement to the result obtained from Chapter III. Both Chapter III's and Chapter V's goals are maximizing the capacity. Chapter III does it from an angle's point of view, while Chapter V does it from a distance's point of view. Combining both techniques on a polar-coordinated 2-dimensional plane will lead to the maximum capacity in the scheme of wireless multi-hop ad hoc access networks.

CHAPTER VI

CONCLUSION

The aim of this dissertation is to analyze the capacity of wireless multi-hop ad hoc access networks with directional antenna. While each chapter builds on top of the other to fulfil the goal, original contributions in each chapter can also stand on their own. The summary of the contributions of each chapter is shown in the following sections, together with suggestion for possible future work.

6.1 Contributions from Chapter III

In Chapter III, the framework in analyzing and maximizing capacity of wireless ad hoc access networks with directional antenna based on a reception condition for a constant data rate is proposed. The novelty of the proposed formula is in the usage of the vector representations. In comparison to other works [34], [35], [36], which add the directional antenna by extending the seminal work [5] straightforwardly without using the vector representations, their conditions are complex and not concise. The proposed unified constraints overcome the complicated and often-confusing directional-based protocol constraints.

The remaining part of Chapter III is dedicated to the multi-hop ad hoc access networks. Using the proposed constraints, the result is meaningfully described as the minimum separable condition. Satisfying this condition can guarantee simultaneous transmissions around a gateway. Finding a proper scheduling to fully utilize the gateway becomes a simple task. Numerical results of different antenna gains are also shown. They can be used to justified the extra cost in deploying directional antenna that has better side-lobe suppression. The results also illustrate that the effect of side lobes is significant and cannot be ignored.

The minimum separation angle proposed in Chapter III can be used as a capacity optimization condition for a dimension of angle in a polar-coordinated 2-dimensional plane. Together with the results from Chapter V, they form a foundation for capacity maximization of the multi-hop ad hoc access networks with directional antenna.

6.2 Contributions from Chapter IV

While Chapter IV provides a stepping stone to Chapter V, many of the findings are noteworthy. Chapter IV shows that, when the reception conditions are relaxed, the capacity bound is described as a continuous function of cumulative interference. In practice, this bound can be achieved by using adaptive modulation and coding that maximizes the capacity in a given environment.

Enabled by certain assumptions, the cumulative interference is found to be conveniently expressed by the concept of equivalent interferers. One of the assumptions made here is uniform random node placement and transmission direction, which is not only widely assumed in literature, but also justifiable in many scenarios. Another assumption made is the cone-plus-ball antenna model. To justify the simplified antenna model, networks with realistic antenna patterns are simulated by Monte Carlo method. The results confirm the validity of the analysis.

The formula obtained in Chapter IV is Shannon capacity of a single hop transmission in a homogeneous environment. The flexibility of the formulation also opens the door for the analysis of multi-hop transmissions in Chapter V.

6.3 Contributions from Chapter V

The extension of single-hop Shannon capacity is the focus of Chapter V. The multi-hop capacity bound of 1-dimensional networks is analytically derived. The capacity bound is found to be achieved by selecting proper intermediate nodes as relays. The criterion for selecting the best relay of each hop is discovered in the form of optimal *SIR* for a particular environment. This has a strong implication in wireless ad hoc routing protocols. Furthermore, the finding of the optimal *SIR* enables a direct comparison between omnidirectional antenna an directional antenna. The benefit of using directional antenna is then analytically expressed.

The optimal relay selection proposed in Chapter V can be used as a capacity optimization condition for a dimension of distance in a polar-coordinated 2-dimensional plane. Together with the results from Chapter III, they form a foundation for capacity maximization of the multi-hop ad hoc access networks with directional antenna.

6.4 Possible Future Work

While the dissertation is self-contained, there are numerous scenarios beyond the scope of this work that could be worth studying. While this dissertation answers the question of relay placement, the question still remains for the **gateway placement**. Moreover, in practice, the question often is not only about where to place a gateway, but how many gateways should be placed. In the **multiple gateways scenario**, while it is obvious that capacity increases with the number of gateways, the balancing act is in the cost of deployment. It then could be formulated as an optimization problem.

Another key performance factor of networks, besides capacity, is **latency**. While, as shown in the dissertation, the multi-hop transmissions can increase the capacity, each hop appends additional latency to the transmissions. Their precise relationship remains open for further investigations.

References

[1] Tseng, Y.-C., Shen, C.-C., and Chen, W.-T. Integrating Mobile IP with Ad Hoc Networks. IEEE Computer 36 , 5 (2003): 48-55+4.

[2] Jönsson, U., Alriksson, F., Larsson, T., Johansson, P., and Jr., G. Q. M., MIPMANET-Mobile IP for Mobile Ad Hoc Networks. Proceedings of ACM MobiHOC'00, (2000): 75-85.

[3] Bölcskei, H., Nabar, R. U., Oyman, O., and Paulraj, A. J. Capacity Scaling Laws in MIMO Relay Networks. IEEE Transactions on Wireless Communications 5 (2006): 1433–1444.

[4] Vilzmann, R. and Bettstetter, C., A Survey on MAC Protocols for Ad Hoc Networks with Directional Antennas. Proceedings of EUNICE Open European Summer School, (2005): 268-274.

[5] Gupta, P. and Kumar, P. R. The Capacity of Wireless Networks. IEEE Transactions on Information Theory 46 (2000): 388–404.

[6] Xue, F. and Kumar, P. R. Scaling Laws for Ad-Hoc Wireless Networks: An Information Theoretic Approach. Foundations and Trends in Networking 1 , 2.

[7] Knuth, D. E. Big Omicron and big Omega and big Theta. SIGACT News 8 , 2 (1976): 18–24.

[8] Li, J., Blake, C., De, D. S. J., Hu, C., Lee, I., and Morris, R., Capacity of Ad Hoc Wireless Networks. Proceedings of the 7th ACM International Conference on Mobile Computing and Networking, (2001): 61–69.

[9] Jain, K., Padhye, J., Padmanabhan, V., and Qiu, L. Impact of interference on Multi-Hop Wireless Network Performance. Wireless Networks 11 , 4 (2005): 471-487.

[10] Kim, T.-S., Lim, H., and Hou, J. C. Understanding and Improving the Spatial Reuse in Multihop Wireless Networks. IEEE Transactions on Mobile Computing 7 , 10 (2008): 1200-1212.

[11] Zemlianov, A. and Veciana, G. Capacity of Ad Hoc Wireless Networks with Infrastructure Support. IEEE Journal on Selected Areas in Communications 23 , 3 (2005): 657-667.

[12] Cho, J.-W., Kim, S.-L., and Chong, S. Capacity of Interference-Limited Ad Hoc Networks with Infrastructure Support. IEEE Communications Letters 10 , 1 (2006): 16-18.

[13] Duarte-Melo, E. J. and Liu, M. Data-Gathering Wireless Sensor Networks: Organization and Capacity. Computer Networks 43 , 4 (2003): 519-537.

[14] Chan, C. P. and Liew, S. C., Data-Collection Capacity of IEEE 802.11-Like Sensor Networks. Proceedings of IEEE ICC'06 7 (2006): 3339-3346.

[15] Ng, P. C., Liew, S. C., and Jiang, L. B., A Performance Evaluation Framework for IEEE 802.11 Ad-Hoc Networks. Proceedings of IEEE PE-WASUN'04, (2004): 123-124.

[16] Ng, P. C., Liew, S. C., and Jiang, L. B., Achieving Scalable Performance in Large-Scale IEEE 802.11 Wireless Networks. Proceedings of IEEE WCNC'05 1 (2005): 69-74.

[17] Jiang, L. B. and Liew, S. C. Improving Throughput and Fairness by Reducing Exposed and Hidden Nodes in 802.11 Networks. IEEE Transactions on Mobile Computing 7 , 1 (2008): 34-49.

[18] Ng, P. C. and Liew, S. C. Throughput Analysis of IEEE802.11 Multi-Hop Ad Hoc Networks. IEEE/ACM Transactions on Networking 15 , 2 (2007): 309-322.

[19] Huang, T.-C. and Wu, S.-Y., An Adaptive Gateway Discovery Algorithm for the Integrated Network of Internet and MANET. Proceedings of ICCNMC'05 3619 (2005): 911-920.

[20] Nordström, E., Gunningberg, P., and Tschudin, C. Comparison of forwarding strategies in internet connected MANETs. SIGMOBILE Mob. Comput. Commun. Rev. 8 , 4 (2004): 72–76.

[21] Ammari, H. M. Lessons Learned from the Simulation Experience of a Three-Tier Multi-Hop Wireless Internet Architecture. Information Sciences 177 , 8 (2007): 1806-1833.

[22] Ruiz, P. M., Ros, F. J., and Gomez-Skarmeta, A. Internet Connectivity for Mobile Ad Hoc Networks: Solutions and Challenges. IEEE Communications Magazine 43 , 10 (2005): 118-125.

[23] Song, J., Wong, V. W. S., and Leung, V. C. M. Efficient On-Demand Routing for Mobile Ad-Hoc Wireless Access Networks. IEEE J. Sel. Areas Commun 22 (2004): 1374–1383.

[24] Huang, C.-F., Lee, H.-W., and Tseng, Y.-C. A Two-Tier Heterogeneous Mobile Ad Hoc Network Architecture and its Load-Balance Routing Problem. Mobile Networks and Applications 9 , 4 (2004): 379-391.

[25] Hsu, C.-Y., Wu, J.-L. C., and Wang, S.-T., Capacity Upgrading in Mobile Ad Hoc Access Networks (MAHANs) using CSMA/CAPA. Proceedings of ACM MobiWAC'06, (2006): 28-34.

[26] Zhou, P., Wang, X., and Rao, R. Asymptotic Capacity of Infrastructure Wireless Mesh Networks. IEEE Transactions on Mobile Computing 7 , 8 (2008): 1011-1024.

[27] Choudhury, R. R. and Vaidya, N. H. Deafness: A MAC Problem in Ad Hoc Networks when using Directional Antennas. Proceedings of ICNP'04 (2004): 283-292.

[28] Choudhury, R. R. and Vaidya, N. H. Performance of Ad Hoc Routing using Directional Antennas. Ad Hoc Networks 3 , 2 (2005): 157-173.

[29] Ramanathan, R., Redi, J., Santivanez, C., Wiggins, D., and Polit, S. Ad Hoc Networking with Directional Antennas: A Complete System Solution. IEEE Journal on Selected Areas in Communications 23 (2005): 496–506.

[30] Hua, Y., Huang, Y., and Garcia-Luna-Aceves, J. Maximizing the Throughput of Large Ad Hoc Wireless Networks. IEEE Signal Processing Magazine 23 , 5 (2006): 84-94.

[31] Peraki, C. and Servetto, S. D., On the Maximum Stable Throughput Problem in Random Networks with Directional Antennas. Proceedings of ACM MobiHOC'03, (2003): 76-87.

[32] Ramanathan, R., On the Performance of Ad Hoc Networks with Beamforming Antennas. Proceedings of ACM MobiHOC'01, (2001): 95-105.

[33] Bazan, O. and Jaseemuddin, M. Multi-Commodity Flow Problem for Multi-Hop Wireless Networks with Realistic Smart Antenna Model, vol. 4982. Springer LNCS, 2008.

[34] Spyropoulos, A. and Raghavendra, C. S., Asympotic Capacity Bounds for Ad-hoc Networks Revisited: The Directional and Smart Antenna Cases. Proceedings of IEEE GLOBECOM'03 3 (2003): 1216-1220.

[35] Spyropoulos, A. and Raghavendra, C. S., Capacity Bounds for Ad-Hoc Networks using Directional Antennas. Proceedings of IEEE ICC'03 1 (2003): 348-352.

[36] Yi, S., Pei, Y., Kalyanaraman, S., and Azimi-Sadjadi, B. How is the Capacity of Ad Hoc Networks Improved with Directional Antennas?. Wireless Networks 13 , 5 (2007): 635-648.

[37] Yu, C., Shin, K. G., and Song, L. Maximizing Communication Concurrency via Link-Layer Packet Salvaging in Mobile Ad Hoc Networks. IEEE Transactions on Mobile Computing 6 , 4 (2007): 449-462.

[38] Kiese, M., Hartmann, C., Lamberty, J., and Vilzmann, R. On Connectivity Limits in Ad Hoc Networks with Beamforming Antennas. EURASIP Journal on Wireless Communications and Networking 2009.

[39] Moser, C., Ad Hoc Networking with Beamforming Antennas: Modeling, Visualization and Connectivity. Master's thesis Technische Universität München Lehrstuhl für Kommunikationsnetze, 2004.

[40] Cai, L. X., Shen, X., and Mark, J. W. Efficient MAC Protocol for Ultra-Wideband Networks. IEEE Communications Magazine 47 , 6 (2009): 179-185.

[41] Ge, Y., Wen, S., Ang, Y.-H., and Liang, Y.-C. Optimal Relay Selection in IEEE 802.16j Multihop Relay Vehicular Networks. IEEE Transactions on Vehicular Technology 59 (jun. 2010): 2198 -2206.

[42] Kim, Y. and Liu, H. Infrastructure Relay Transmission With Cooperative MIMO. IEEE Transactions on Vehicular Technology 57 (jul. 2008): 2180 -2188.

Appendix

Appendix

List of Publications

Komolkiti, P. and Aswakul, C.

"Maximizing Concurrent Transmissions in Wireless Ad Hoc Access Networks with Directional Antenna", appeared in 2008 International Workshop on Smart Info-Media Systems in Bangkok (SISB 2008), Okinawa, Japan. Content taken from Chapter II and Chapter III

"Interference-Based Capacity Analysis of Wireless Ad Hoc Networks with Directional Antenna", submitted to the IEEE Communications Letters, under review. Content taken from Chapter II and Chapter IV

Biography

Patrachart Komolkiti was born in 1975 in Bangkok, Thailand. He received the Bachelor of Engineering with Honor from Chulalongkorn University, Bangkok, Thailand, in 1997, and the Master of Science in Electrical and Computer Engineering from Northwestern University, Evanston, Illinois, USA, in 1998. He has been pursuing the Doctoral degree in Electrical Engineering at Chulalongkorn University, Bangkok, Thailand, since 2005. His research interests include Wireless Networks, Vehicular Networks, and Intelligent Transportation Systems.